第67卷 第3期 地 质 论 评 GEOLOGICAL REVIEW Vol. 67 No. 3
2021年5月 May, 2021

贺根山缝合带阿萨格图钾玄质火山岩锆石LA-ICP-MS U-Pb年龄、地球化学特征及构造意义

Pre-pub. on line: www.geojournals.cn/georev

王金芳,李英杰,李红阳,董培培
河北地质大学地球科学学院,石家庄,050031

内容提要:内蒙古西乌珠穆沁旗阿萨格图火山岩出露于贺根山缝合带迪彦庙蛇绿混杂岩南侧,岩石类型为粗安岩、粗面岩和粗面英安岩。粗安岩锆石LA-ICP-MS U-Pb同位素测年获得火山岩形成年龄为132.1±0.7Ma。岩石地球化学显示火山岩属于钾玄岩系列,岩石高Na_2O+K_2O(7.61%~10.35%)、高K_2O(3.94%~6.04%)、高Al_2O_3(16.32%~17.99%)、低TiO_2(0.45%~0.95%),富集Rb、Ba、U等大离子亲石元素(LILE)和轻稀土元素(LREE),亏损Nb、Ta和Ti等高场强元素(HFSE)。稀土元素含量为109.62×10^{-6}~174.68×10^{-6},稀土元素配分曲线为右倾式分布。岩石学和岩石地球化学特征表明,阿萨格图地区白垩纪火山岩与洋壳俯冲作用有关,形成于俯冲板片断离—后造山伸展构造背景。古亚洲洋俯冲洋壳析出流体交代上覆地幔形成贺根山缝合带富集地幔,随后的俯冲板片断离—后造山伸展作用触发富集地幔部分熔融产生该钾玄质岩浆。结合贺根山缝合带的壳幔电性结构和晚古生代蛇绿岩—岛弧岩浆岩、中生代后造山A型花岗岩的时空分布与演化,初步建立了该区钾玄质火山岩的板片断离—后造山伸展地球动力学模式。

关键词:钾玄质火山岩;板片断离;后造山伸展环境;早白垩世;贺根山缝合带

钾玄质火山岩为富碱高钾的钾玄质系列岩石,主要包括钾玄岩、粗面玄武岩、玄武粗安岩、粗安岩、安粗岩和粗面岩等,主要见于与俯冲作用有关的初始洋弧、晚期洋弧、大陆弧和后碰撞环境(Morrison, 1980;Müller et al., 1992;Foley et al., 1992;邱检生等,2003;Squire et al., 2007;Pe-Piper et al., 2014;贾小辉等,2017)。在化学成分上,钾玄质火山岩富碱($K_2O+Na_2O>5\%$)、高钾($K_2O/Na_2O>0.5$)、低钛($TiO_2<1.3\%$)、铝含量高而范围大($Al_2O_3=14\%$~19%)、高Fe_2O_3/FeO值(>0.5),富集大离子亲石元素(K、Rb、Sr、Ba等)和轻稀土,亏损高场强元素(Nb、Ta、Ti等)(Morrison, 1980;Müller et al., 1992,2000;Foley et al., 1992;邱检生等,2003;尼玛次仁等,2015;Xue Huaimin et al., 2015;王良玉等,2016)。一般认为,造山带环境下的钾玄质火山岩主要起源于与俯冲作用有关的俯冲板片析出流体(富钾和大离子亲石元素)交代地幔,多记录着与俯冲作用有关的俯冲板块物质演变与岩浆作用过程信息,兼有壳幔双重特殊地球化学特征和特定成因指示意义。因此,钾玄质岩一直是岩浆岩研究领域和地质学研究中的重要课题之一(Wyborn, 1992;Aftabi et al., 2000;Jiang Yaohui et al., 2002;Ding Lixue et al., 2011;李世超等,2013;邱检生等,2013;Conticelli et al., 2015;王良玉等,2016)。在造山带的构造演化过程研究中,识别和研究与俯冲作用有关而形成于后碰撞环境的钾玄质火山岩,可为判别俯冲板片断离—后造山伸展拉张构造演化提供岩石学证据与时间约束。

内蒙古中部二连—贺根山缝合带(图1a)广泛分布中生代火山岩(图1b,图2),其与晚古生代蛇绿岩—岛弧岩浆岩、中生代A型花岗岩的时空分布及其成因联系(图1b,图2),已逐渐成为国内外地质工作者关注和研究的科学问题之一(张晓晖等,2006;李可等,2012;张学斌等,2015;李红英等,

注:本文为国家自然科学基资助项目"内蒙古迪彦庙蛇绿岩带前弧玄武岩组合及其成因"(编号:41972061)、中国地质调查局项目"内蒙古1::5万高力罕牧场三连等四幅区调"(编号:1212011120711)和"内蒙古1∶5万沙日勒昭等四幅区调"(编号:1212011120701)的成果。
收稿日期:2020-01-23;改回日期:2021-03-07;网络首发:2021-03-20;责任编辑:章雨旭。Doi:10.16509/j.georeview.2021.03.075
作者简介:王金芳,女,1983年生,副教授,主要从事岩石学和地球化学研究;Email:wjfb1983@163.com。

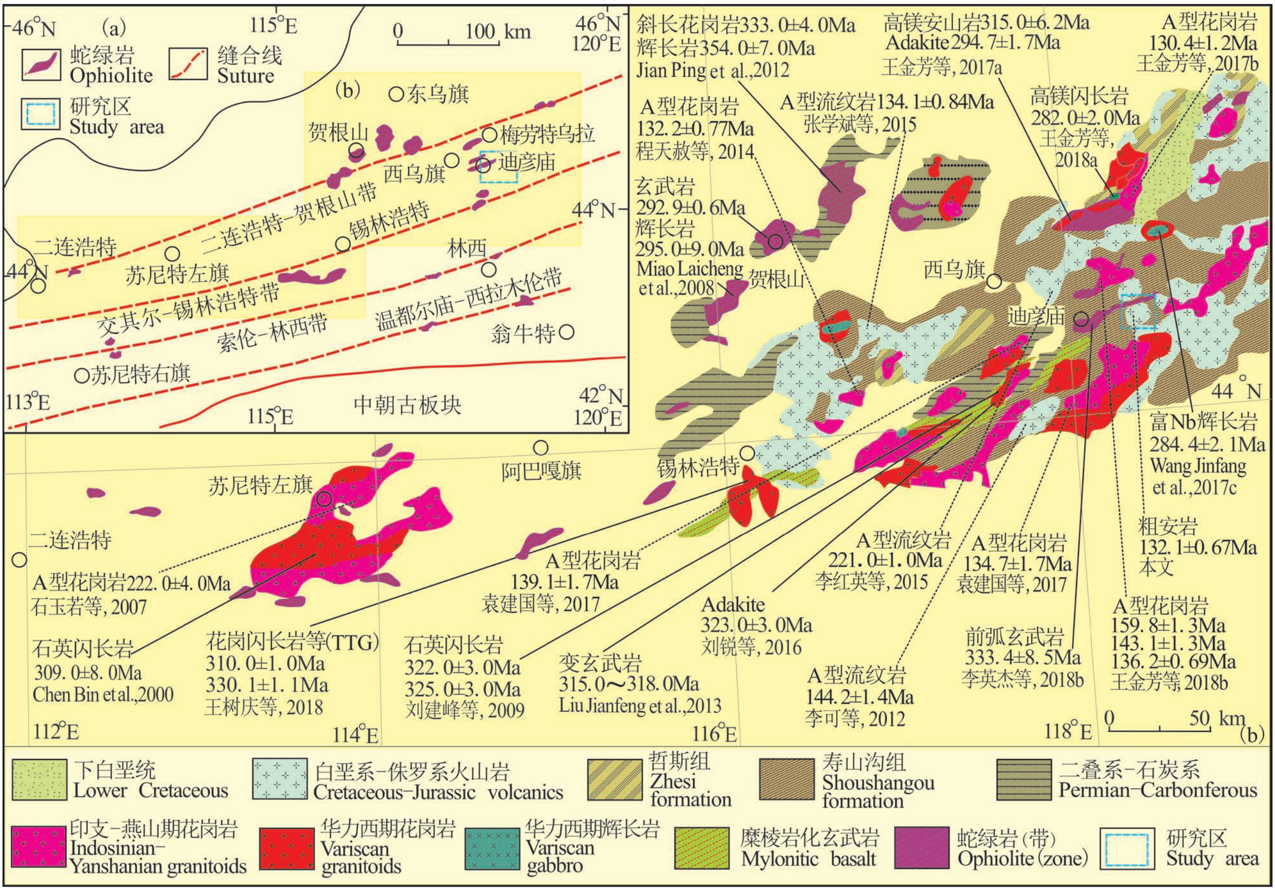

图 1 二连—贺根山缝合带区域构造(a)和地质简图(b)

Fig. 1 Sketch tectonic map (a) and regional geological map (b) of the Erenhot—Hegenshan suture zone

2015;程银行等,2016;王金芳等,2020b)。

与晚古生代蛇绿岩—岛弧岩浆岩和中生代 A 型花岗岩相比,对二连—贺根山缝合带中生代火山岩的研究还比较薄弱(Sengor et al., 1993;陈斌等,2001;Windley et al., 2007;石玉若等,2007;Miao Laicheng et al., 2008;Xiao Wenjiao et al., 2009;Jian Ping et al., 2012;Liu Jianfeng et al., 2013;Zhang Zhicheng et al., 2015;李钢柱等,2017;Li Yingjie et al., 2018a;王金芳等,2018,2020b),尤其缺乏钾玄质火山岩锆石 U-Pb 年代学、地球化学、成因和构造环境的系统研究,在一定程度上制约了我们对二连—贺根山缝合带俯冲—碰撞缝合—后造山伸展构造演化的认识。

为此,本文在 1∶5 万沙日勒昭等四幅区域地质矿产调查的基础上,选择西乌珠穆沁旗迪彦庙蛇绿混杂岩带南侧阿萨格图地区新识别出的钾玄质火山岩进行锆石 U-Pb 年代学、地球化学和构造环境研究,并结合二连—贺根山缝合带晚古生代蛇绿岩—岛弧岩浆岩、中生代后造山 A 型岩浆岩和贺根山缝合带壳幔电性结构特征相关研究成果,探讨区内钾玄质火山岩岩浆作用与二连—贺根山缝合带古亚洲洋俯冲板片断离—后造山伸展拉张作用的深部地球

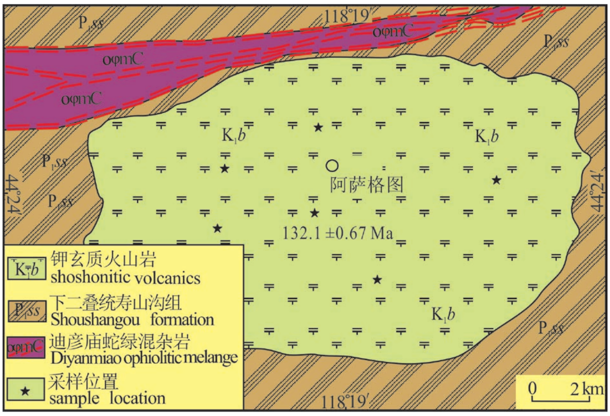

图 2 西乌珠穆沁旗阿萨格图火山岩地质简图

Fig. 2 Geological map of volcanic rocks in Asagetu area, West Ujimqin Banner

动力学过程,为中亚造山带东段二连—贺根山缝合带构造演化研究提供新的证据。

1　区域地质概况和岩石学特征

内蒙古西乌旗阿萨格图火山岩,位于二连—贺根山缝合带东段迪彦庙蛇绿混杂岩带南侧(图 1b,图 2)。研究区内出露的地层主要为中生界下白垩统白音高老组火山岩和上古生界下二叠统寿山沟组复理石沉积(图 1b,图 2)。白音高老组火山岩出露面积约 140 km^2,厚度约 280 m,由 4 个破火山机构组成较完整的阿萨格图火山盆地。对区内这套火山岩的岩性和时代归属,1∶20 万白塔子庙幅区域地质调查[1]将其划归为上侏罗统上兴安岭组酸性火山岩,1∶25 万西乌旗幅[2]将其归为上侏罗统满克头鄂博组酸性火山岩,缺少地球化学和年代学等资料。本文最新的锆石 LA-ICP-MS U-Pb 测定结果表明,该套火山岩的形成时代为早白垩世,将其归属于下白垩统白音高老组二段火山岩。

1∶5 万沙日勒昭幅区域地质矿产调查表明,阿萨格图地区白音高老组二段火山岩以粗安岩(图 3a—d)为主,少量粗面岩(图 3e、f)和粗面英安岩,局部可见少量粗安质火山角砾岩(图 3g、h)、粗安质含角砾熔结凝灰岩和粗安质含角砾凝灰岩等火山碎屑岩。火山熔岩呈浅灰色、灰紫色和灰绿色,斑状结构(图 3a—f),块状构造(图 3a),气孔、杏仁构造(图 3 c、d)。岩石常见多斑、聚斑结构,斑晶主要为斜长石(图 3b、d),少量透长石(图 3f),基质多为交织结构、微晶结构和粗面结构。其中,粗安岩主要包括多斑粗安岩(图 3a、b)和杏仁状粗安岩(图 3c、d)。多斑粗安岩:浅灰色和灰紫色,斑状结构,块状构造,斑晶主要为斜长石(15%~25%),可见聚斑晶形态,粒度 0.4~6 mm,大者达 10 mm。斜长石呈半自形板状,零散分布,其类型主要为中长石;基质为隐晶质,粒度一般小于 0.5 mm,主要由斜长石、钾长石和暗色矿物假象(角闪石)组成,长英质矿物呈微晶粗面结构, 交织状分布。可见不透明矿物呈浸染状分布。副矿物组合为磁铁矿、磷灰石、锆石和钛铁矿。

杏仁状粗安岩:浅灰色和灰绿色,斑状结构,杏仁状构造,斑晶主要为斜长石(15%~25%),可见聚斑晶形态,粒度 0.5~6 mm,大者达 10 mm。斜长石呈半自形板状零散分布,主要为中长石(图 3d),可见绢云母化和碳酸盐化;基质为隐晶质,粒度一般小于 0.5 mm,主要为斜长石、钾长石和火山玻璃,长英质矿物呈微晶似粗面结构,交织状分布,粒径一般< 0.25 mm。暗色矿物呈半自形—他形粒状,填隙状分布于斜长石粒间。玻璃质呈黑褐色,零星充填于斜长石间,部分脱玻为纤状雏晶,并析出少量铁质。可见近圆状、不规则状气孔星散分布,大小一般 0.1 ~2 mm 不等,部分被绿泥石、硅质、碳酸盐和褐铁矿等充填,形成杏仁体(8%~15%)。

2　测试方法

2.1　锆石 U-Pb 测年

本文锆石 U-Pb 测年样品采自西乌旗阿萨格图地区火山岩中的粗安岩,样品编号为 PTC22-1,采样地理位置为 N44°22′48.0″ E118°17′57.4″(图 2)。

粗安岩(PTC22-1)中锆石样品分选工作在河北省区域地质调查研究所完成。样品经粉碎、磁选和重选分选出纯度较高的锆石, 然后在双目镜下挑选出无色透明晶形好、无明显裂痕的测年锆石(图 4)。锆石样品制靶和透射光、反射光、阴极发光照相在北京锆年领航科技有限公司完成。LA-ICP-MS 锆石 U-Pb 年龄测试在天津地质调查中心完成,使用仪器为 Neptune 多接收电感耦合等离子体质谱仪和 193 nm 激光取样系统(LA-MC-ICP-MS)。分析中采用的激光剥蚀斑束为 35 μm,能量密度为 13~14 J/cm,频率为 8~10 Hz,激光剥蚀物质以 He 为载气送入 Neptune(MC-ICP-MS)。锆石标样采用 TEMORA 标准锆石。普通 Pb 的校正采用 Anderson 方法(Andersen, 2002)进行, 锆石 U-Pb 年龄加权平均值采用 ISOPLOT 程序计算完成(表 1)。

2.2　岩石地球化学测试分析

本次研究工作在阿萨格图地区火山岩中采集了 6 件地球化学样品, 主量和微量元素分析在河北省区域地质矿产研究所完成。样品按照常规方法首先在破碎机上进行粗碎,然后在玛瑙钵体和柱头研磨机上研磨至 200 目。主量元素用 X 射线荧光光谱仪(Axiosmax)分析,微量元素分析采用电感耦合等离子体质谱分析 (ICP-MS)测定。主量和微量元素测试分析结果如表 2。

3　测试结果

3.1　锆石 U-Pb 年代学

粗安岩样品 LA-ICP-MS 锆石 U-Pb 同位素分析结果见表 1,单颗粒锆石的阴极发光图像 (CL)、测点和年龄值如图 4。粗安岩(PTC22-1)样品的 25 颗锆石晶体多呈自形—半自形双锥状或短柱状,发育


(a)
(b)
Pl
Pl
Pl
Pl
Pl
Pl
1mm
(c)
(d)
Pl
Pl
Pl
Pl
1mm
(e)
(f)
San
1mm
(g)
(h)
1mm

图 3 贺根山缝合带阿萨格图钾玄质火山岩野外和显微照片:(a) 块状粗安岩;(b) 交织结构;(c) 杏仁状粗安岩;(d) 杏仁状构造;(e) 粗面岩;(f) 斑状结构;(g) 粗安质火山角砾岩;(h) 火山角砾结构

Fig. 3 Representative field photos and photomicrograph of the Asagetu shoshonitic volcanic rocks in the Hegenshan Suture: (a) massive trachyandesite; (b) pilotaxitic texture; (c) amygdaloidal trachyandesite; (d) amygdaloidal structure; (e) trachyte; (f) porphyritic texture; (g) trachyandesitic volcanic breccia; (h) volcanic breccia texture

Pl —斜长石;San —透长石

Pl —plagioclaae;San —sanidine

较明显的振荡生长环带, 反映了中性岩浆成因锆石特征。

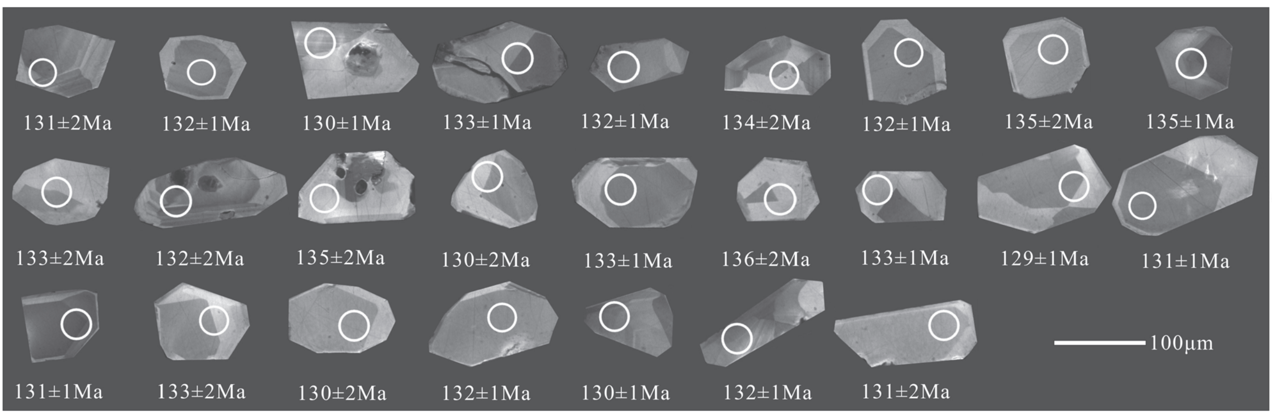

图 4 贺根山缝合带阿萨格图钾玄质火山岩(PTC22-1)锆石阴极发光图像及其 $n(^{206}Pb)/n(^{238}U)$ 年龄

Fig. 4 Cathodoluminescent images and $n(^{206}Pb)/n(^{238}U)$ ages of zircons from Asagetu shoshonitic volcanic rocks in the Hegenshan Suture

粗安岩(PTC22 -1)样品锆石的 Th/U 值为 0.23~0.40, 平均值为 0.32, 为岩浆成因锆石(Claesson et al., 2000;Corfu et al., 2003)。25 颗锆石测点的 $n(^{206}Pb)/n(^{238}U)$ 表面年龄位于 U-Pb 谐和图上或其附近(图 5), 加权平均年龄为 132.1±0.7Ma(n=25, MSWD=1.2), 代表粗安岩的岩浆结晶年龄。因此,本区白音高老组火山岩属早白垩世。

3.2　主量元素

主量元素分析结果如表 2。该区火山岩的 SiO_2 含量为 60.40%~65.59%,平均 62.71%;全碱含量高,Na_2O+K_2O 为 7.61%~10.35%,平均 9.06%;K_2O 含量高,为 3.94%~6.04%,平均 4.91%;相对富钾,K_2O/Na_2O 为 0.93~1.45,平均 1.19;Al_2O_3 含量为 16.32%~17.99%,平均 17.16%;而 TiO_2 含量为 0.45%~0.95%,平均 0.70%;全铁含量相对较低,Fe_2O_3+FeO 为 3.50%~5.60%, 平均 4.74%;MgO 含量较低, 为 0.47%~2.19%,平均 1.14%。该区火山岩样品的 A/CNK 值为 1.12~1.21,A/NK 值为 1.14~1.25,属于过铝质岩石。

在 TAS 火山岩分类图解中(图 6a),该区火山岩有 3 个样品落在碱性系列区,另外 3 个样品落在碱性和亚碱性系列分界线附近。在 K_2O—Na_2O 图中(图 6b)(Miller et al.,1999),6 个样品均落在钾玄质区域。在 SiO_2—K_2O 岩浆系列硅碱判别图解中(图 6c)(Peccerillo et al.,1976),6 个样品也均落于钾玄岩系列区域,表明该区火山岩为钾玄质岩石。

3.3　稀土元素

稀土元素分析结果如表 2。岩石的稀土总量相对较低,为 110×10^{-6}~175×10^{-6},平均 143×10^{-6}。轻重稀土分馏明显,LREE/HREE 比值为 3.30~5.18,平均 3.91;$(La/Yb)_N$ 为 7.33~11.75,平均 8.33,属轻稀土富集型。在稀土元素球粒陨石标准化配分图上(图 7a),6 个样品具有近于一致的轻稀土元素富集的右倾分布模式(图 7a,表 2),可能反映了同源岩浆演化特征。这些样品的轻稀土元素和重稀土元素内部也均表现出明显的分馏,$(La/Sm)_N$ 为 2.58~3.80,平均 3.07,$(Gd/Yb)_N$ 为 1.60~1.97,平均 1.78,而且,分馏程度总体随原子序数的增加而降低,表现出配分曲线近于平坦(图 7a)。δEu 为

表 1 贺根山缝合带阿萨格图钾玄质火山岩(PTC22--1)LA-ICP-MS 锆石 U-Pb 测试结果

Table 1 LA-ICP-MS U-Pb dating results of zircons from the Asagetu shoshonitic volcanic rocks in the Hegenshan Suture

测点号	元素含量($\times10^{-6}$)			Th/U	同位素比值						同位素年龄(Ma)						谐和度(%)
	Pb	Th	U		$n(^{207}Pb)/n(^{206}Pb)$		$n(^{207}Pb)/n(^{235}U)$		$n(^{206}Pb)/n(^{238}U)$		$n(^{207}Pb)/n(^{206}Pb)$		$n(^{207}Pb)/n(^{235}U)$		$n(^{206}Pb)/n(^{238}U)$		
					测值	1σ	测值	1σ	测值	1σ	测值	1σ	测值	1σ	测值	1σ	
1	2	27	81	0. 33	0. 0550	0. 0037	0. 1562	0. 0140	0. 0206	0. 0003	412	151	145	13	131	2	90. 34
2	2	24	70	0. 35	0. 0469	0. 0041	0. 1341	0. 0120	0. 0208	0. 0002	42	211	128	11	132	1	96. 97
3	1	14	43	0. 33	0. 0531	0. 0044	0. 1493	0. 0149	0. 0204	0. 0002	333	189	141	14	130	1	92. 20
4	2	24	97	0. 25	0. 0541	0. 0048	0. 1557	0. 0142	0. 0209	0. 0002	374	199	147	13	133	1	90. 48
5	2	18	74	0. 24	0. 0528	0. 0037	0. 1505	0. 0150	0. 0207	0. 0002	321	159	142	14	132	1	92. 96
6	1	17	52	0. 32	0. 0532	0. 0048	0. 1539	0. 0184	0. 0210	0. 0002	337	203	145	17	134	2	92. 41
7	2	25	72	0. 34	0. 0511	0. 0050	0. 1459	0. 0121	0. 0207	0. 0002	247	227	138	11	132	1	95. 65
8	1	17	47	0. 37	0. 0468	0. 0042	0. 1361	0. 0109	0. 0211	0. 0003	38	213	130	10	135	2	96. 30
9	3	33	140	0. 24	0. 0479	0. 0035	0. 1401	0. 0105	0. 0212	0. 0002	93	174	133	10	135	1	98. 52
10	1	13	45	0. 29	0. 0541	0. 0045	0. 1550	0. 0127	0. 0208	0. 0003	375	188	146	12	133	2	91. 10
11	2	24	93	0. 26	0. 0496	0. 0047	0. 1418	0. 0184	0. 0207	0. 0003	175	221	135	17	132	2	97. 78
12	1	9	37	0. 25	0. 0526	0. 0048	0. 1538	0. 0127	0. 0212	0. 0003	311	206	145	12	135	2	93. 10
13	1	12	42	0. 29	0. 0521	0. 0049	0. 1464	0. 0121	0. 0204	0. 0003	290	215	139	11	130	2	93. 53
14	2	34	101	0. 34	0. 0540	0. 0049	0. 1546	0. 0148	0. 0208	0. 0002	370	203	146	14	133	1	91. 10
15	1	17	51	0. 33	0. 0563	0. 0041	0. 1654	0. 0139	0. 0213	0. 0002	464	160	151	13	136	2	90. 07
16	2	25	99	0. 26	0. 0520	0. 0050	0. 1497	0. 0146	0. 0209	0. 0002	287	219	142	14	133	1	93. 66
17	1	18	54	0. 34	0. 0541	0. 0044	0. 1508	0. 0133	0. 0202	0. 0002	375	185	143	13	129	1	90. 21
18	2	30	81	0. 37	0. 0516	0. 0048	0. 1466	0. 0122	0. 0206	0. 0002	269	215	139	12	131	1	94. 24
19	3	46	129	0. 36	0. 0516	0. 0037	0. 1465	0. 0104	0. 0206	0. 0002	269	164	139	10	131	1	94. 24
20	1	16	46	0. 34	0. 0513	0. 0051	0. 1470	0. 0138	0. 0208	0. 0003	254	227	139	13	133	2	95. 68
21	1	20	51	0. 40	0. 0514	0. 0047	0. 1445	0. 0118	0. 0204	0. 0002	259	212	137	11	130	2	94. 89
22	1	23	59	0. 38	0. 0533	0. 0042	0. 1519	0. 0118	0. 0207	0. 0002	344	179	144	11	132	1	91. 67
23	3	32	140	0. 23	0. 0493	0. 0038	0. 1382	0. 0108	0. 0204	0. 0002	160	182	131	10	130	1	99. 24
24	4	62	166	0. 37	0. 0501	0. 0027	0. 1433	0. 0078	0. 0207	0. 0002	199	127	136	7	132	1	97. 06
25	1	18	50	0. 36	0. 0534	0. 0052	0. 1509	0. 0119	0. 0205	0. 0003	347	222	143	11	131	2	91. 61

注:误差为 1σ;Pb* 指示放射成因铅。实验测试在天津地质矿产研究所完成。

表 2 贺根山缝合带阿萨格图钾玄质火山岩的主量、微量和稀土元素分析结果

Table 2 Major element, trace element and REE analyses of the Asagetu shoshonitic volcanic rocks in the Hegenshan Suture

样品号	PTC21	PTC22	PTC23	PTC24	PTC25	PTC26	样品号	PTC21	PTC22	PTC23	PTC24	PTC25	PTC26
岩性	粗安岩	粗安岩	粗安岩	粗面岩	粗面岩	粗面英安岩	岩性	粗安岩	粗安岩	粗安岩	粗面岩	粗面岩	粗面英安岩
SiO_2	60.40	61.29	62.18	63.23	63.58	65.59	Zr	304	370	329	469	512	453
TiO_2	0.95	0.88	0.72	0.60	0.59	0.45	Hf	5.98	8.83	6.46	10.8	10.9	13.3
Al_2O_3	16.32	17.38	16.68	17.99	17.68	16.93	Cs	12.2	5.66	6.04	4.60	6.80	3.19
Fe_2O_3	2.53	1.29	2.79	2.61	2.42	2.16	Th	8.16	6.68	8.41	5.26	3.24	8.82
FeO	3.07	4.10	2.13	1.86	2.11	1.34	U	2.65	1.04	2.66	1.75	1.74	2.28
MnO	0.090	0.120	0.090	0.070	0.050	0.060	Y	22.3	16.8	23.5	14.4	16.7	17.1
MgO	2.19	1.52	1.37	0.67	0.63	0.47	La	32.0	19.8	30.7	22.2	20.6	34.5
CaO	4.33	3.18	3.56	0.76	0.36	0.90	Ce	68.7	43.0	67.5	42.7	51.3	76.4
Na_2O	3.67	4.43	4.04	4.43	3.98	4.31	Pr	8.81	6.02	8.71	5.57	6.63	9.21
K_2O	3.94	4.11	4.27	5.34	5.78	6.04	Nd	34.4	24.4	34.2	21.7	26.4	33.7
P_2O_5	0.32	0.20	0.22	0.16	0.16	0.13	Sm	6.56	4.82	6.47	4.12	4.94	5.71
烧失	1.95	1.04	1.70	2.07	2.35	1.43	Eu	1.79	1.68	1.66	1.34	1.24	1.20
总量	99.76	99.54	99.75	99.79	99.69	99.81	Gd	5.12	4.44	5.12	3.62	3.88	4.53
$Mg^{\#}$	42	34	34	22	21	20	Tb	0.841	0.650	0.853	0.572	0.644	0.682
Rb	94.7	56.0	97.0	108	116	135	Dy	4.37	3.44	4.52	3.11	3.43	3.56
Ba	1183	1340	1426	1690	1645	950	Ho	0.841	0.640	0.870	0.622	0.661	0.683
Sr	541	386	429	293	167	206	Er	2.26	1.81	2.44	1.74	1.79	1.85
Cr	45.5	15.6	26.4	15.4	8.38	7.42	Tm	0.384	0.303	0.402	0.270	0.311	0.301
Co	13.1	0	8.22	0	5.74	3.07	Yb	2.19	1.82	2.59	1.78	1.81	1.98
Ni	7.74	0	6.87	0	3.57	3.34	Lu	0.584	0.290	0.663	0.282	0.431	0.371
Pb	14.0	0	13.9	0	12.9	18.3	ΣREE	169	113	167	110	124	175
Nb	13.0	7.08	12.1	7.68	9.38	9.89	δEu	0.913	1.092	0.851	1.040	0.842	0.701
Ta	0.840	0.510	0.990	0.580	0.780	0.930	$(La/Yb)_N$	9.85	7.33	8.00	8.41	7.65	11.7

注:主量元素含量单位为%,稀土、微量元素含量为 10^{-6}。

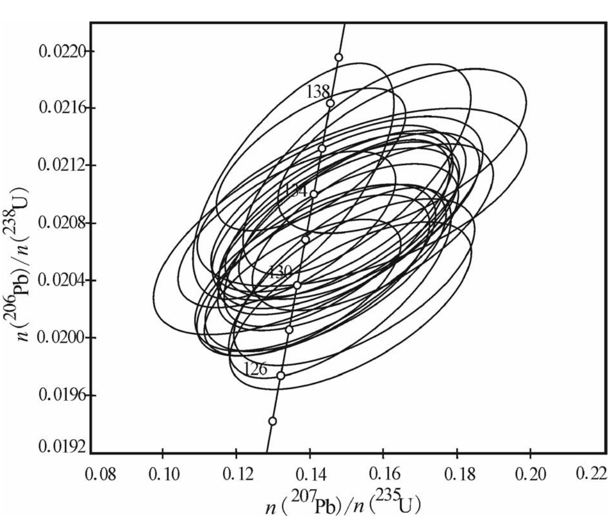

图 5 贺根山缝合带阿萨格图钾玄质火山岩(PTC22-1)锆石 U-Pb 谐和图

Fig. 5 U-Pb concordia diagram of zircons from the Asagetu shoshonitic volcanic rocks in the Hegenshan Suture

0.7,1~1.092,平均 0.907,总体表现为微弱 Eu 负异常特征。

3.4　微量元素

如表 2 和图 7b 所示,在微量元素特征上,本区火山岩明显富集 Rb、Ba、U 等大离子亲石元素(LILE),亏损 Nb、Ta、Ti 和 P 等高场强元素(HFSE),Nb—Ta—Sr—P—Ti 负异常显著(图 7b),Zr 和 Hf 相对富集。其中,Rb 含量为 56.0×10^{-6} ~ 135×10^{-6},Ba 含量为 950×10^{-6} ~ 1690×10^{-6},U 含量为 1.04×10^{-6} ~ 2.66×10^{-6}, Nb 含量为 7.08×10^{-6} ~ 13.0×10^{-6},Ta 含量为 0.510×10^{-6} ~ 0.990×10^{-6}。在原始地幔标准化微量元素蛛网图上(图 7b),6 个样品总体具有近于一致的微量元素右倾式分布曲线,明显的 Nb、Ta、Sr、P、Ti 负异常和 Zr、Hf 正异常。此外,该区火山岩具有明显较高的 Ce/Yb (23.6 ~ 38.6)和 Ta/Yb (0.28 ~ 0.47)比值,在 Ce/Yb—Ta/Yb 图解中(图 8)(Müller et al., 1992),6 个样品样品均投影在钾玄质系列范围内,与主量元素 K_2O—

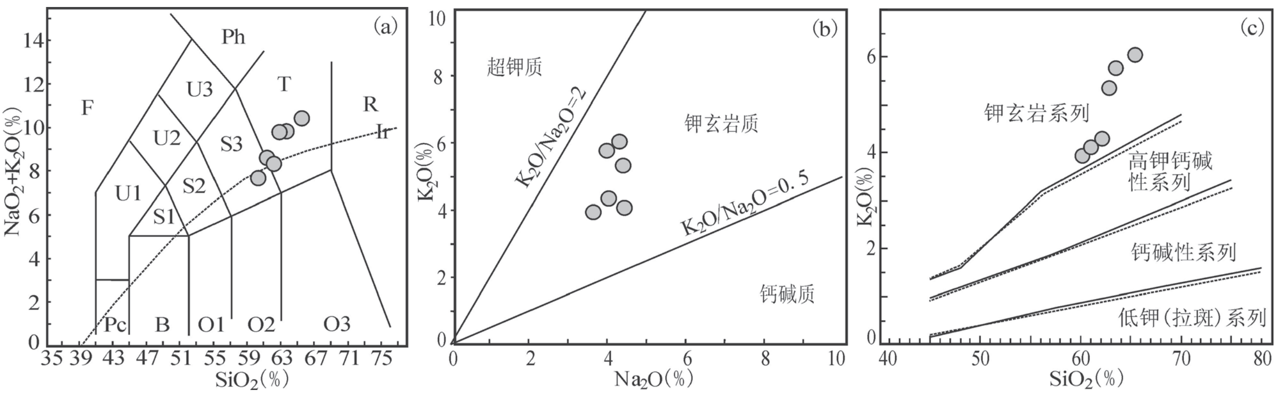

图 6 贺根山缝合带阿萨格图钾玄质火山岩岩石化学分类判别图解(a,据 Peccerillo et al. ,1976; b,据 Miller et al. ,1999;c,据 Middlemost,1994)

Fig. 6 Petrochemical classification and discrimination diagrams of the Asagetu shoshonitic volcanic rocks in the Hegenshan Suture (a,after Middlemost,1994;b,after Miller et al. ,1999;c,after Peccerillo et al. ,1976)

T—粗面岩、粗面英安岩; S3—粗面安山岩

T—trachyte, trachy dacite; S3—trachy andesite

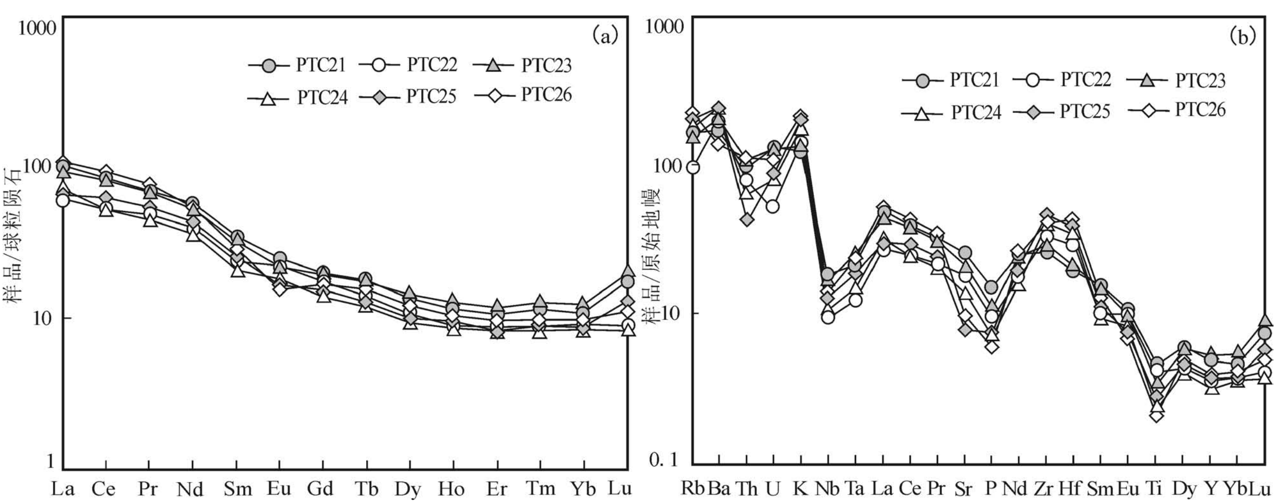

图 7 贺根山缝合带阿萨格图钾玄质火山岩稀土元素球粒陨石标准化配分模式 (a, 据 Boynton, 1984)和微量元素原始地幔标准化蛛网图 (b, 据 Sun and McDonough, 1989)

Fig. 7 Chondrite-normalized REE distribution patterns(a, after Boynton,1984) and primitive mantle-normalized trace elements spider diagram(b, after Sun and McDonough, 1989) of the Asagetu shoshonitic volcanic rocks in the Hegenshan Suture

Na_2O 和 SiO_2—K_2O 判别结果相吻合，表明该区火山岩为钾玄质岩石。

4 讨论

4.1 岩石属性、源区特征及成因

阿萨格图火山岩高碱 Na_2O+K_2O(7.61%~10.35%)、高 K_2O(3.94%~6.04%)、高 K_2O/Na_2O 值(0.93~1.45)，高 Al_2O_3(16.32%~17.99%)、低 TiO_2(0.45%~0.95%)，富集 Rb、Ba、U 等大离子亲石元素(LILE)和轻稀土元素(LREE)，亏损 Nb、Ta 和 Ti 等高场强元素(HFSE)。在相关图解上投影于钾玄岩图区，表明其岩石类型属于钾玄质岩石(Morrison, 1980; Müller et al., 1992; Foley et al., 1992; Turner et al., 1996; Williams et al., 2004; 章邦桐等, 2011; 邱检生等, 2002, 2013; Xue Huaimin et al., 2015; Jahangiri et al., 2016)。与此同时，该区火山岩具有较高的 Th/Ta(4.15~13.10)、Th/Nb(0.35~0.94)、Ba/Nb(90.96~220.05)和 Ce/Nb(5.28~7.72)值，反映岩浆源区经历了流体交代作用过程，表明岩浆源区为早期俯冲作用释放流体交

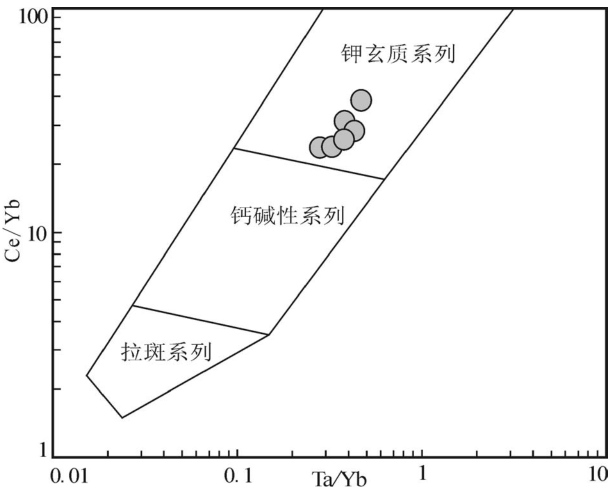

图 8 贺根山缝合带阿萨格图钾玄质火山岩 Ce/Yb—Ta/Yb 图解(据 Müller et al., 1992)

Fig. 8 Ce/Yb—Ta/Yb diagram for the Asagetu shoshonitic volcanic rocks in the Hegenshan Suture (after Müller et al., 1992)

代而富集的地幔源区(Pearce et al., 1995;Elliott et al., 1997;Zhang Zhaochong et al., 2008)。

在 Ce/Yb 对 Cs/Rb、Ba/La 和 U/Th 地幔流体交代作用判别图解上(图 9),该区火山岩 6 个样品的 Cs/Rb、Ba/La 和 U/Th 值变化范围明显较大,呈现出与地幔流体交代作用趋向线基本一致的变化趋势,进一步提供了该区火山岩形成过程中有早期俯冲作用释放流体交代作用参与的地球化学证据(李曙光等,1997;Sun Chihhsien et al., 2001;邱检生等, 2003,2013;章邦桐等,2011)。

在 $(La/Sm)_N$—$(Ba/La)_N$ 图解上(图 10),本区火山岩 6 个样品均位于深海沉积物区域内,反映俯冲洋壳+俯冲深海沉积物析出流体进入地幔参与了成岩过程,更进一步揭示了本区钾玄质火山岩的源区性质(Othman et al., 1989;Jiang Yaohui et al., 2002;邱检生等, 2003, 2013;Conticelli et al., 2015)。

实验研究表明,俯冲洋壳中少量富钾沉积物在一定温度压力下可产生超钾质流体(Massonne, 1992;邱检生等,2003)。这些流体上升渗透到上覆地幔中并交代地幔而形成富钾的富集地幔(Massonne,1992;邱检生等,2003)。这种与俯冲作用有关的富集地幔在后期构造—热事件中部分熔融产生钾玄质岩浆。前人研究揭示,钾玄质火山岩中尖晶石橄榄岩捕虏体内含有少量富钾的金云母和角闪石等含水矿物,其可能反映了俯冲板片析出富钾流体的交代作用及产物(邱检生等,2003)。这种来自富集地幔包体中的金云母富 K、Sr、Ba、Rb,贫 Th、HFSE 和 REE,K/Rb 值为 40~400;而角闪石具有相对较高的 K、Sr、Ba、HFSE、LREE 含量和较低的 Rb、Th 含量,K/Rb 值>1100(Chakrabarti et al., 2009)。而且,金云母分解形成的熔体 Rb/Sr 值较高(>0.1),Ba/Rb 值较低(<20)(Furman et al, 1999)。

本区钾玄质火山岩的 REE 和 HFSE 含量明显较低,K/Rb 比值也明显较低(345~609,平均 419);而 Rb/Sr 比值明显较高(0.15~0.69,平均 0.38);Ba/Rb 比值明显较低(7.0~23.9,平均 14.7),表明其岩浆来源与金云母密切相关。这些特征反映研究

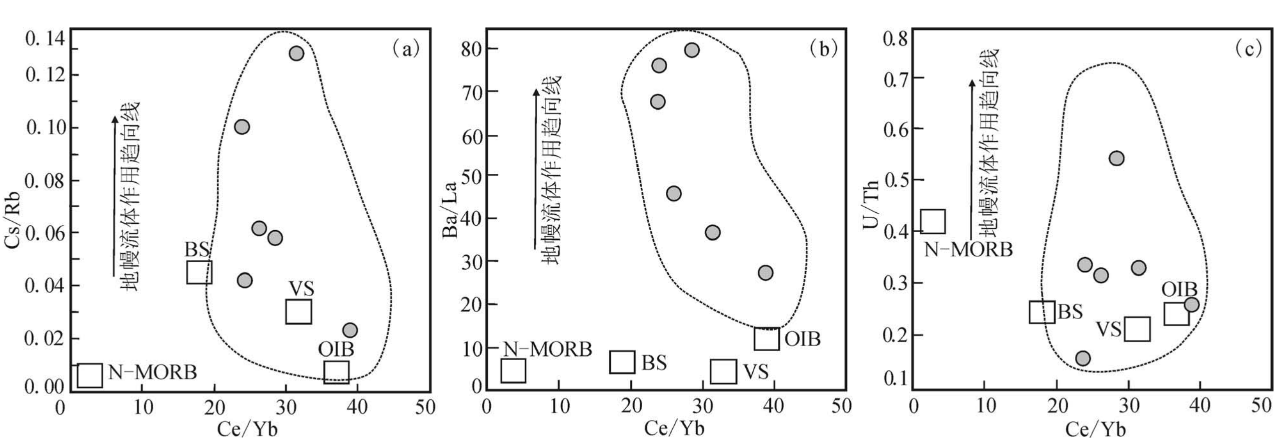

图 9 贺根山缝合带阿萨格图钾玄质火山岩 Ce/Yb 对 Cs/Rb (a)、Ba/La (b) 和 U/Th (c)图解(据 Sun et al., 2001)

Fig. 9 Cs/Rb (a), Ba/La (b) and U/Th (c) vs. Ce/Yb diagrams of the Asagetu shoshonitic volcanic rocks in the Hegenshan Suture (after Sun et al., 2001)

N-MORB—N 型洋脊玄武岩;OIB—洋岛玄武岩;VS—火山碎屑沉积物;BS—全部沉积物

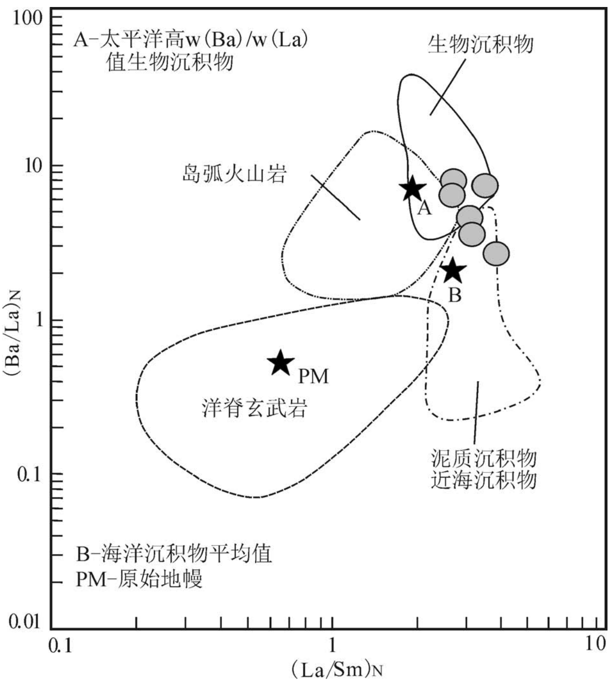

图 10 贺根山缝合带阿萨格图钾玄质火山岩（La/Sm)$_N$—(Ba/La)$_N$ 图解(据 Othman et al., 1989)

Fig. 10 (La/Sm)$_N$—(Ba/La)$_N$ diagram of the Asagetu shoshonitic volcanic rocks in the Hegenshan Suture (after Othman et al., 1989)

区钾玄质火山岩可能源于含金云母的富集地幔,也表明金云母可能是本区富集地幔源区的主要富钾含水矿物。这种含金云母的富集地幔部分熔融产生了该区的钾玄质岩浆(Sun et al., 1989;Furman et al, 1999;Ebert et al., 2004;Zhang Zhaochong et al., 2008)。

该区钾玄质火山岩的地幔源区特征,与邻区西乌旗那木斯来敖包晚侏罗世粗面岩同位素低[$n(^{87}Sr)/n(^{87}Sr)]_i$(0.7037、0.7036)、高 $\varepsilon_{Nd}(t)$(6.36、7.39)和低 T_{DM} 值(362、296Ma)所反映的地幔源区特征相吻合(李可等,2012);与苏尼特左旗红格尔早白垩世钾玄质火山岩同位素正 $\varepsilon_{Nd}(t)$(+0.40~+1.64)和低 T_{DM} 值(694~767Ma)反映的地幔源区特征相类似(张祥信等,2016);并与整个贺根山缝合带中生代火成岩 Sr—Nd 同位素正 $\varepsilon_{Nd}(t)$ 和低 T_{DM} 值所反映的岩浆源区特征基本一致(张晓晖等,2006;李可等,2012;张祥信等,2016)。而且,邻区西乌旗扎布其尔沃布勒吉—杰林牧场一带广泛发育早白垩世橄榄玄武岩、玄武安山岩和杏仁—气孔状玄武安山岩(薛晓刚等,2018),其岩浆源区为富集地幔,可能进一步揭示了贺根山缝合带晚侏罗世—早白垩世幔源钾玄质岩浆事件。

因此,本区钾玄质火山岩岩浆源区可能是古亚洲洋俯冲洋壳+俯冲深积物析出流体交代地幔而形成的含金云母二辉橄榄岩,而随后的古亚洲洋俯冲板片断离—后造山伸展作用下诱发含金云母的二辉橄榄岩部分熔融而产生本区的钾玄质火山岩岩浆(Sun et al., 1989; Massonne, 1992; Furman et al, 1999; Jiang Yaohui et al., 2002; 邱检生等, 2003; Ebert et al., 2004; Zhang Zhaochong et al., 2008; Conticelli et al., 2015;杨华本等,2016)。

然而,与富集地幔部分熔融产生的岩浆 SiO_2 含

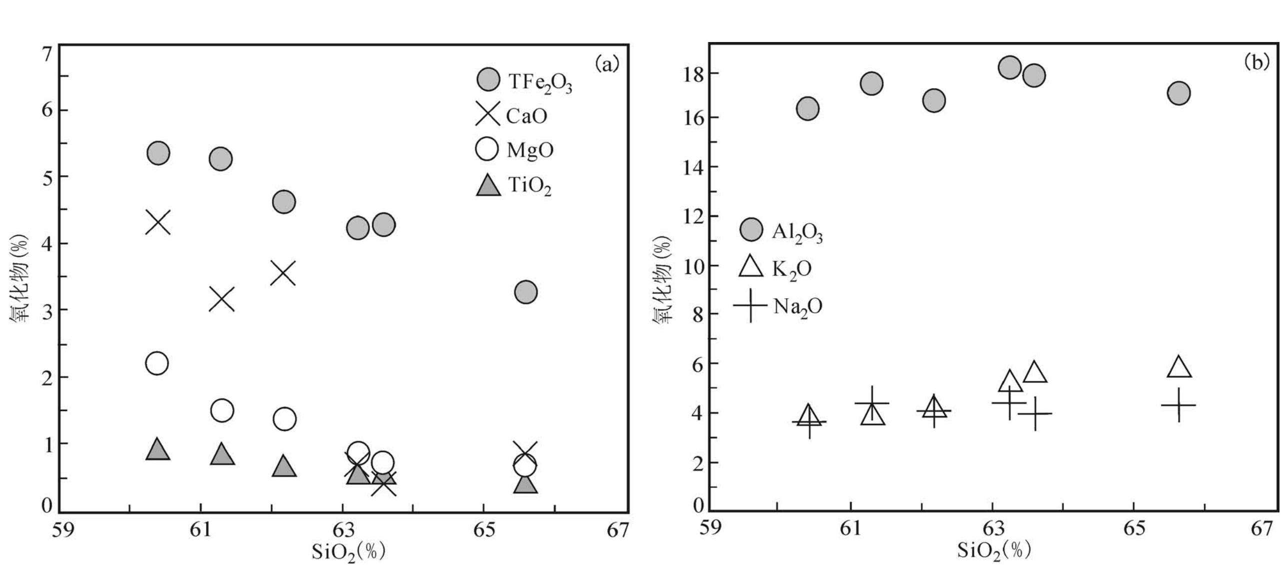

图 11 贺根山缝合带阿萨格图钾玄质火山岩 SiO_2—氧化物关系图

Fig. 11 SiO_2 versus oxide diagrams of the Asagetu shoshonitic volcanic rocks in the Hegenshan Suture

量普遍较低相对比,本区钾玄质火山岩 SiO_2 含量明显较高(60.40%~65.59%),可能反映其岩浆经历了分离结晶作用过程。在 SiO_2—氧化物关系图上(图 11),本区火山岩的 TFe_2O_3、CaO、MgO、TiO_2、K_2O 等主要氧化物含量与 SiO_2 均呈明显的线性变化关系,而 Al_2O_3 和 Na_2O 含量则基本未发生明显规律性变化,反映了同源岩浆分离结晶演化的特征。其中,TFe_2O_3、CaO、MgO、TiO_2 与 SiO_2 呈明显负相关,K_2O 与 SiO_2 呈正相关,Al_2O_3、Na_2O 与 SiO_2 相关性不明显,表明岩浆演化过程中存在钛铁矿、磁铁矿、角闪石、斜长石、磷灰石分离结晶。从岩相学上,该区钾玄质火山岩发育多斑、聚斑结构,斑晶主要为斜长石,少量角闪石,其副矿物组合为磁铁矿+磷灰石+锆石+钛铁矿,也反映了岩浆经历了分离结晶作用过程。

该区火山岩的 MgO 含量(0.47%~2.19%)、$Mg^{\#}$值(20~42)和 Cr($7.42\sim45.5\times10^{-6}$)、Co($3.07\sim13.1\times10^{-6}$)、Ni($3.34\sim7.74\times10^{-6}$)含量均较低,而且伴随 SiO_2 含量的增高而降低,可能较好地反映了该区钾玄质岩浆经历了铁镁矿物的分离结晶作用过程。而且,一般认为重稀土元素在铁镁矿物中的分配系数远大于轻稀土元素,铁镁矿物的分离结晶作用通常导致熔体中重稀土含量降低,或$(La/Yb)_N$比值增大。该区火山岩$(La/Yb)_N$比值与 SiO_2 含量总体为正相关关系(表 2),可能同样反映了铁镁矿物的分离结晶作用。在微量元素原始地幔标准化蛛网图上(图 7b),该区火山岩的微量元素 Ti 和 P 显示强烈的亏损,某种程度上可能主要反映钾玄质岩浆经历了钛铁矿、磷灰石和榍石的分离结晶作用。在另一方面,该区火山岩的 δEu 值(0.701~1.092)与 Sr 含量($167\times10^{-6}\sim541\times10^{-6}$)为正相关关系(表 2),表现出伴随 Eu 负异常的增大而 Sr 含量降低,可能较好地揭示该区钾玄质岩浆作用过程中斜长石的分离结晶作用。而且,该区火山岩的 La/Sm 比值(4.11~6.04)伴随 La 含量的增大(19.8~34.5)总体相对稳定,表明岩浆分离结晶作用在该区钾玄质岩浆演化与成岩过程中的重要作用。

综上所述,阿萨格图钾玄质火山岩可能是由地幔的钾玄质岩浆经铁镁矿物、斜长石、钛铁矿和磷灰石的分离结晶作用形成。

4.2 构造环境与意义

钾玄质火山岩可以形成于初始洋弧、晚期洋弧、大陆弧、后造山和板内等不同的大地构造环境,被广泛应用于古构造环境的恢复与研究(Morrison,1980;Müller et al., 1992;Williams et al., 2004;Ding Lixue et al., 2011;邱检生等,2013;尼玛次仁等,2015;王良玉等,2016;Jahangiri et al., 2016)。在钾玄质岩的 Zr/Al_2O_3—TiO_2/Al_2O_3 构造环境判别图解上(图 12a),本区钾玄质火山岩 6 个样品均落在大陆弧—后造山钾玄质岩范围内,明显区别于初始洋弧、晚期

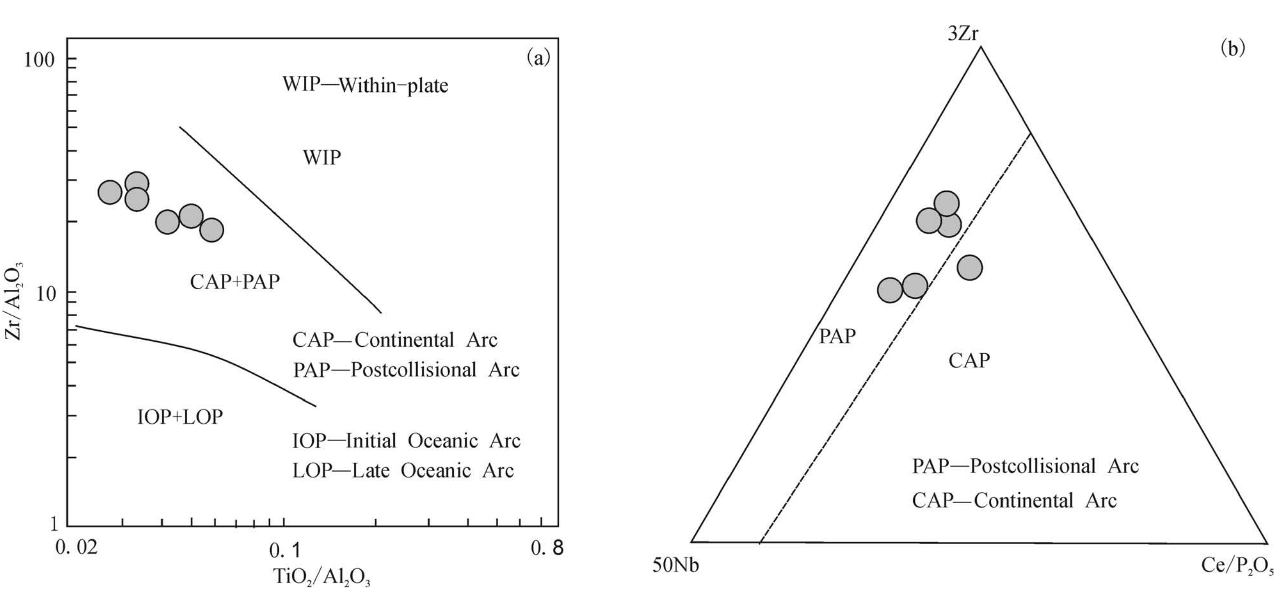

图 12 贺根山缝合带阿萨格图钾玄质火山岩 Zr/Al_2O_3—TiO_2/Al_2O_3(a)和 3Zr—50Nb—Ce/P_2O_5(b)判别图解(据 Müller et al., 1992)

Fig. 12 Zr/Al_2O_3—TiO_2/Al_2O_3(a) and 3Zr—50Nb—Ce/P_2O_5(b) discrimnation diagrams of the Asagetu shoshonitic volcanic rocks in the Hegenshan Suture (after Müller et al., 1992)

洋弧和板内型钾玄质岩。在大陆弧和后造山钾玄质岩 $3Zr—50Nb—Ce/P_2O_5$ 三角形构造环境判别图解中(图 12b)，该区钾玄质火山岩有 5 个样品落在后造山钾玄质岩范围，1 个样品投影在后造山与大陆弧钾玄质岩分界线附近的大陆弧一侧，表明其应形成于后造山构造环境，为与后造山相关的钾玄质岩。这种后造山钾玄质岩的伸展构造环境，可与国内外典型后造山钾玄质岩石相类比(Morrison, 1980; Müller et al., 1992; Turner et al., 1996; 邱检生等, 2002; Williams et al., 2004; Zhang Zhaochong et al., 2008; Jahangiri et al., 2016; 杨华本等, 2016)。

在区域构造—岩浆演化研究上，近十年来中亚造山带东段二连—贺根山缝合带区域内获得大量有关石炭纪蛇绿岩、石炭纪—二叠纪岛弧岩浆岩和三叠纪—早白垩世后造山 A 型花岗岩—酸性火山岩等岩石学、地球化学和年代学成果。虽然一些学者提出古亚洲洋最终闭合时间可能为晚白垩世(吕洪波等, 2018)；但是，越来越多的证据表明古亚洲洋可能在二叠纪晚期闭合，华北板块和西伯利亚板块可能在二叠纪末(最晚至早三叠世)最终碰撞缝合，二连—贺根山缝合带在中三叠世—早白垩世处于古亚洲洋俯冲板片断离—后造山伸展拉张构造背景(Miao Laicheng et al., 2008; Xiao Wenjiao et al., 2009; 刘建峰等, 2009; Jian Ping et al., 2010, 2012; Liu Jianfeng et al., 2013; Zhang Zhicheng et al., 2015; 康健丽等 2016; 刘锐等, 2016; 李钢柱等, 2017; 王树庆等, 2018; 汪相, 2018; 范玉须等, 2019; 王金芳等, 2019, 2020a, 2021)。本文报道的阿萨格图后造山钾玄质火山岩，分布于二连—贺根山缝合带石炭纪蛇绿岩、石炭纪—二叠纪岛弧岩浆岩和三叠纪—早白垩世后造山 A 型花岗岩—酸性火山岩典型发育区，其直接上覆于早石炭世迪彦庙蛇绿混杂岩带和下二叠统寿山沟组复理石(俯冲增生杂岩)之上(李英杰等, 2012, 2015, 2018b; Wang Jinfang et al., 2017; 王金芳等, 2017a, 2018c; Li Yingjie et al., 2018c)，新获得的 LA-ICP-MS 锆石 U-Pb 年龄为 132.1±0.7Ma，表明其形成于早白垩世。该火山岩的形成年龄与二连—贺根山缝合带三叠纪—早白垩世后造山阶段 A 花岗岩、酸性火山岩的年龄范围(245～130Ma)一致(刘红涛等, 2002; 邓晋福等, 2015a; 张晓晖等, 2006; 石玉若等, 2007; 程天赦等, 2014; 张学斌等, 2015; 李红英等, 2015; 程银行等, 2016; 袁建国等, 2017; 王金芳等, 2017b, 2018b)。

通常认为，钾玄质火山岩的形成时间相对较晚，主要为构造—岩浆活动演化晚期产物，在空间分布上往往位于地层层序的上部或顶部层位，代表与先前洋壳俯冲作用有关而形成于后造山伸展拉张晚期的岩浆作用产物(Morrison, 1980; Müller et al., 1992, 2000; 邱检生等, 2003, 2013; 邓晋福等, 2015b)。结合区域内石炭纪蛇绿岩、石炭纪—二叠纪岛弧岩浆岩和三叠纪—早白垩世俯冲板片断离—后造山 A 型花岗岩—酸性火山岩的时空分布、成因联系与演化关系，本区早白垩世后造山钾玄质火山岩代表了贺根山缝合带后造山阶段的晚期岩浆作用产物，进一步揭示了贺根山缝合带在二叠纪末俯冲—碰撞造山事件结束后进入俯冲板片断离—后造山伸展拉张构造演化阶段。而且，也正是伴随古亚洲洋在二叠纪末(最晚至早三叠世)洋壳俯冲与闭

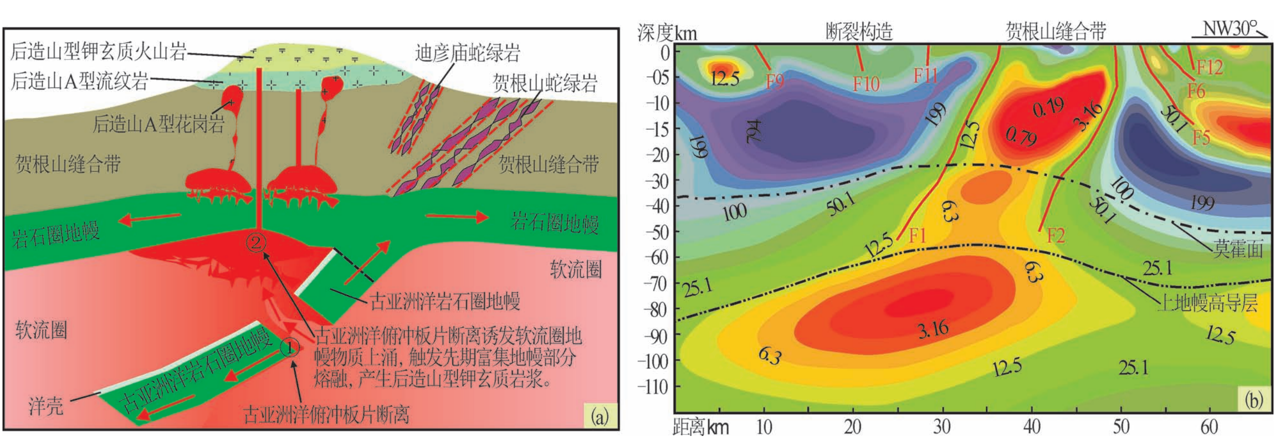

图 13 贺根山缝合带钾玄质火山岩的俯冲板片断离—后造山伸展地球动力学模式(a)和壳幔电性结构特征(b)((b)据徐新学等, 2011)

Fig. 13 The geodynamic model of the subducted slab break off—post orogenic extension of the shoshonitic volcanic rocks (a) and the crust—upper mantle electrical structure (b) in the Hegenshan Suture Zone (b, after Xu Xinxue et al., 2011#)

合,俯冲的洋壳+俯冲深积物析出流体交代上覆地幔形成贺根山缝合带富集地幔,进而随后的俯冲板片断离引发软流圈物质沿板片断离产生的"板片窗"上涌(图 13a),触发先期富集地幔减压部分熔融形成后造山钾玄质岩浆(图 13a)。对于本区后造山钾玄质火山岩的地球动力学背景和过程(图 13a),贺根山缝合带的壳幔电性结构特征可能提供一些重要佐证(图 13b)(徐新学等,2011)。贺根山缝合带内的 3 个串珠状巨型高导块体和上地幔高导层隆起区(图 13b)(徐新学等,2011),较好地表征了俯冲板片断离(古亚洲洋残留块体)、软流圈物质上涌触发富集地幔减压部分熔融(后造山钾玄质岩浆作用)(图 13a,b),反映贺根山缝合带具有明显的壳幔高导层连通渠道(图 13b),是幔源物质向上运移的通道(徐新学等,2011),可能为二连—贺根山缝合带先期古亚洲洋壳俯冲—闭合、俯冲板片断离—后造山伸展地球动力学过程提供了新的佐证。

5　结论

(1) 贺根山缝合带西乌旗阿萨格图地区白音高老组二段火山岩以粗安岩为主,少量粗面岩和粗面英安岩,岩石高碱 Na_2O+K_2O、高 K_2O、高 Al_2O_3、低 TiO_2,富集 Rb、Ba、U 等大离子亲石元素(LILE)和轻稀土元素(LREE),亏损 Nb、Ta 和 Ti 等高场强元素(HFSE),属于典型的钾玄质岩。

(2) 贺根山缝合带阿萨格图地区白音高老组二段火山岩中的粗安岩,LA-ICP-MS 锆石 U-Pb 年龄为 132.1±0.7Ma,提供了二连—贺根山缝合带早白垩世后造山钾玄质岩浆作用的岩石学和年代学证据与约束。

(3) 阿萨格图钾玄质火山岩与古亚洲洋俯冲作用有关,形成于随后的俯冲板片断离—后造山伸展环境,为与后造山相关的钾玄质岩。古亚洲洋俯冲洋壳+俯冲深积物析出流体交代上覆地幔形成贺根山缝合带富集地幔,随后的俯冲板片断离作用和软流圈物质上涌触发富集地幔部分熔融,产生后造山钾玄质岩浆及其随后的铁镁矿物、斜长石、钛铁矿和磷灰石的分离结晶作用。

(4) 结合贺根山缝合带的壳幔电性结构特征和晚古生代蛇绿岩—岛弧岩浆岩、中生代后造山 A 型岩浆岩的时空分布与演化,认为区域早白垩世处于古亚洲洋俯冲板片断离—后造山伸展构造背景。

致谢:审稿专家和责任编辑为本文提供了宝贵的修改意见与建议,对本文的改进和提高起到了重要作用,在此表示衷心的感谢!

注　释 / Notes

❶ 辽宁省第二区域地质测量队. 1972. 1∶200000 地质图说明书,L-50-35(白塔子庙幅).

❷ 沈阳地质矿产研究所. 2004. 1∶250000 区域地质调查报告,L50C004003(西乌珠穆沁旗幅).

参　考　文　献 / References

(The literature whose publishing year followed by a "&" is in Chinese with English abstract; The literature whose publishing year followed by a "#" is in Chinese without English abstract)

陈斌,赵国春, Wilde S. 2001. 内蒙古苏尼特左旗南两类花岗岩同位素年代学及其构造意义. 地质论评, 47(4):361~367.

程天赦,杨文静,王登红. 2014. 内蒙古西乌旗阿鲁包格山 A 型花岗岩锆石 U-Pb 年龄、地球化学特征及地质意义. 大地构造与成矿学, 38(3):718~728.

程银行,李影,刘永顺,滕学建,李艳锋,杨俊泉,奥琮. 2016. 松辽盆地西缘早白垩世伸展事件:流纹岩锆石 U-Pb 年龄、地球化学研究. 地质学报, 90(12):3492~3507.

邓晋福,冯艳芳,狄永军,刘翠,肖庆辉,苏尚国,赵国春,孟斐,车如凤. 2015a. 古亚洲构造域侵入岩时——空演化框架. 地质论评, 61(6):1211~1224.

邓晋福,冯艳芳,狄永军,刘翠,肖庆辉,苏尚国,赵国春,孟斐,马帅,姚图. 2015b. 岩浆弧火成岩构造组合与洋陆转换. 地质论评, 61(03):473~484.

范玉须,李廷栋,肖庆辉,程杨,李岩,郭灵俊,罗鹏跃. 2019. 内蒙古西乌珠穆沁旗晚二叠世花岗岩的锆石 U-Pb 年龄、地球化学特征及其构造意义. 地质论评, 65(1):248~266.

贾小辉,王晓地,杨文强,牛志军. 2017. 钾玄质系列岩石的研究现状. 地质论评, 63(6):1587~1601.

康健丽,肖志斌,王惠初. 2016. 内蒙古锡林浩特早石炭世构造环境:来自变质基性火山岩的年代学和地球化学证据. 地质学报, 90(2):383~397.

李钢柱,王玉净,李成元. 2017. 内蒙古索伦山蛇绿岩带早二叠世放射虫动物群的发现及其地质意义. 科学通报, 62(5):400~406.

李红英,周志广,张达,李鹏举. 2015. 内蒙古西乌旗格尔楚鲁晚三叠世流纹岩年代学、地球化学特征及其地质意义. 矿物岩石地球化学通报, 34(3):546~555.

李可,张志诚,李建锋,汤文豪,冯志硕,李秋根. 2012. 内蒙古西乌珠穆沁旗地区中生代中酸性火山岩 SHRIMP 锆石 U-Pb 年龄和地球化学特征. 地质通报, 31(5):671~685.

李世超,徐仲元,刘正宏,李永飞. 2013. 大兴安岭中段玛尼吐组火山岩 LA-ICP-MS 锆石 U-Pb 年龄及地球化学特征. 地质通报, 32(Z1):399~407.

李曙光,聂永红,肖益林,郑永飞,Jagoutz E. 1997. 大别山俯冲陆壳的再循环——地球化学证据. 中国科学(D 辑), 27(5):412~418.

李英杰,王金芳,李红阳,董培培. 2012. 内蒙古西乌旗迪彦庙蛇绿岩的识别. 岩石学报, 28(4):1282~1290.

李英杰,王金芳,李红阳,董培培. 2015. 内蒙古西乌旗梅劳特乌拉蛇绿岩的识别. 岩石学报, 31(5):1461~1470.

李英杰,王金芳,王根厚,李红阳,董培培. 2018b. 内蒙古迪彦庙蛇绿岩带达哈特前弧玄武岩的发现及其地质意义. 岩石学报,34(2):469~482.

刘红涛,翟明国,刘建明,孙世华. 2002. 华北克拉通北缘中生代花岗岩:从碰撞后到非造山. 岩石学报, 18(4):433~448.

刘建峰,迟效国,张兴洲. 2009. 内蒙古西乌旗南部石炭纪石英闪长岩地球化学特征及其构造意义. 地质学报, 83(3):365~376.

刘锐,杨振,徐启东,张晓军,姚春亮. 2016. 大兴安岭南段海西期花岗岩类锆石 U-Pb 年龄、元素和 Sr — Nd — Pb 同位素地球化学:岩石成因及构造意义. 岩石学报,32(05):1505~1528.

吕洪波,冯雪东,王俊,朱晓青,董晓朋,张海春,章雨旭. 2018. 狼山发现蛇绿混杂岩——华北克拉通与中亚造山带碰撞边界的关键证据. 地质论评, 64(4):777~805.

尼玛次仁,王国灿,顿都,次仁央宗. 2015. 西藏狮泉河地区高钾—钾玄质火山岩的岩石学、地球化学及锆石 U-Pb 年龄. 地质通报, 34(09):1656~1667.

邱检生,刘亮,李友连,赵姣龙. 2013. 沂沭断裂带中南段钾质火山岩的元素地球化学与 Sr—Nd—Hf 同位素组成及其对岩石成因的制约. 地质学报,87(09):1193~1210.

邱检生,王德滋,刘洪,凌文黎. 2002,大别造山带北缘后碰撞富钾火山岩:地球化学与岩石成因. 岩石学报,(03): 319~330.

邱检生,徐夕生,蒋少涌. 2003. 地壳深俯冲与富钾火山岩成因. 地学前缘, 10(3):191~200.

石玉若,刘敦一,张旗. 2007. 内蒙古中部苏尼特左旗地区三叠纪 A 型花岗岩锆石 SHRIMP U-Pb 年龄及其区域构造意义. 地质通报, 26(2):183~189.

田树刚,李子舜,张永生,宫月萱,翟大兴,王猛. 2016. 内蒙东部及邻区晚石炭世——二叠纪构造古地理环境及演变. 地质学报, 90 (4):688~707.

汪相. 2018. 白云鄂博超大型稀土—铌—铁矿床的成矿时代及成因探析——兼论 P — T 之交生物群灭绝事件和“阿蒙兴造山运动”. 地质论评, 64(2):299~345.

王金芳,李英杰,李红阳,董培培. 2018b. 内蒙古西乌旗石匠山晚侏罗世——早白垩世 A 型花岗岩锆石 U-Pb 年龄及构造环境. 地质通报,37 (2~3):382~396.

王金芳,李英杰,李红阳,董培培. 2018a. 内蒙古梅劳特乌拉蛇绿岩中早二叠世高镁闪长岩的发现及洋内俯冲作用. 中国地质, 45 (4):706~719.

王金芳,李英杰,李红阳,董培培. 2018c. 内蒙古乌兰沟埃达克岩锆石 U-Pb 年龄及构造环境. 地质通报,37(10): 1933~1943.

王金芳,李英杰,李红阳. 2017a. 内蒙古梅劳特乌拉蛇绿岩中埃达克岩的发现及其演化模式. 地质学报,91(08): 1776~1795.

王金芳,李英杰,李红阳. 2017b. 内蒙古西乌旗努和特早白垩世 A 型花岗岩 LA-ICP-MS 锆石 U-Pb 年龄及其地质意义. 地质通报, 36 (8):1343~1358.

王金芳,李英杰,李红阳,董培培. 2019. 贺根山缝合带白音呼舒奥长花岗岩锆石 U-Pb 年龄、地球化学特征及构造意义. 地质论评, 65(4):857~872.

王金芳,李英杰,李红阳,董培培. 2020a. 古亚洲洋晚石炭世俯冲作用:梅劳特乌拉蛇绿岩中扎嘎音高镁安山岩证据. 地质论评,66 (2):289~306.

王金芳,李英杰,李红阳,董培培. 2020b. 古亚洲洋俯冲板片断离与后造山伸展:贺根山缝合带火山岩年代学和地球化学证据. 地质学报,94(12):3561~3580.

王金芳,李英杰,李红阳,董培培. 2021. 贺根山缝合带晚石炭世 TTG 岩浆事件:奥长花岗岩锆石 U-Pb 年龄和地球化学制约. 地质学报,95(2):396~412.

王良玉,廖群安,江云川,罗婷,胡朝斌,肖典,汤帅,刘洋. 2016. 内蒙古锡林浩特早白垩世晚期钾玄质火山岩成因及构造环境. 地质通报, 35(06):919~931.

王树庆,胡晓佳,杨泽黎,赵华雷,张永,郝爽,何丽. 2018. 兴蒙造山带中段锡林浩特跃进地区石炭纪岛弧型侵入岩年代学、地球化学、Sr—Nd—Hf 同位素特征及其地质意义. 地球科学, 43(3):1~31.

徐新学,李俊健,刘俊昌,辛建伟,代涛,牛永强,张丽. 2011. 内蒙古锡林浩特——东乌旗剖面壳幔电性结构研究. 地球物理学报, 54 (5):1301~1309.

薛晓刚, 周长红, 张学斌, 李彩虹. 2018. 内蒙古锡林郭勒盟东部梅勒图组火山岩锆石 U-Pb 年龄、地球化学特征及其地质意义. 地质与勘探, 54 (5):957~967.

杨华本,王文东,闫永生,魏小勇,耿成宝. 2016. 大兴安岭北段新林区塔木兰沟组火山岩成因及地幔富集作用. 地质论评,62 (6): 1471~1486.

袁建国,任永健,姜振宁,屈云燕,魏浩. 2017. 内蒙古锡林浩特毛登牧场早石炭世花岗岩锆石 U-Pb 年龄、地球化学特征及其地质意义. 现代地质, 31(06):1131~1146.

张晓晖,张宏福,汤艳杰. 2006. 内蒙古中部锡林浩特——西乌旗早三叠世 A 型酸性火山岩的地球化学特征及其地质意义. 岩石学报, 22(11):2769~2780.

张祥信, 高永丰, 雷世和. 2016. 内蒙古中部红格尔地区玛尼吐组钾玄质火山岩锆石 U-Pb 年龄、地球化学及其地质意义. 地球化学, 45 (4) :356~373.

张学斌,周长红,来林,徐翠,田颖,陈丽贞,魏民. 2015. 锡林浩特东部早白垩世白音高老组岩石地球化学特征、LA-MC-ICP-MS 锆石 U-Pb 年龄及地质意义. 地质与勘探, 51(02):290~302.

章邦桐,吴俊奇,凌洪飞,陈培荣. 2011. 板内橄榄玄粗岩(shoshonite)地幔流体交代作用及成因的元素地球化学证据:以赣南会昌橄榄玄粗岩为例. 地球化学, 40(5):443~453.

Aftabi A & Atapour H. 2000. Regional aspects of shoshonitic volcanism iniran. Episodes, 23(2):119~125.

Andersen T. 2002. Correction of commen lead U-Pb analyses that do not report ^{204}Pb. Chemical Geology,192: 59~79.

Boynton W V. 1984. Geochemistry of the rare earth elements: meteorite studies. In: Henderson P. eds. Rare Earth Element Geochemistry. Amsterdam: Elsevier: 63~114.

Chakrabarti R, Basu A R, Santo A P, Tedesco D, Vaselli O. 2009. Isotopic and geochemical evidence for a heterogeneous mantle plume origin of the Virunga volcanics, Western rift, East African Rift system. Chem. Geol., 259: 273~289.

Chen Bin, Jahn Bor-ming, Wilde S, Xu Bei. 2000. Two contrasting Paleozoic magmatic belts in northern Inner Mongolia, China: petrogenesis and tectonic implications. Tectonophysics,328: 157~182.

Chen Bin,Zhao Guochun, Wilde S. 2001&. Subduction and collision — related granitoids from southern Sonidzuoqi, Inner Mongolia:Isotopic ages and tectonic implication. Geological Review,47 (4): 361~367.

Cheng Tianshe, Yang Wenjing and Wang Denghong. 2014&. Zircon U-Pb age and geochemical characteristics of the Alubaoge A-type granite in Xiwuqi, Inner Mongolia and its geological significance. Geotectonica et Metallogenia,38(3):718~728.

Cheng Yinhang, Li Ying, Liu Yongshun, Teng Xuejian, Li Yanfeng, Yang Junquan, Ao Cong. 2016&. The tectonic extensional event during the Early Cretaceous in the west margin of Songliao Basin: U-Pb dating, geochemistry and petrogenesis of rhyolites. Acta Geologica Sinica, 90(12):3492~3507.

Claesson S, Vetrin V, Bayanova T. 2000. U-Pb zircon age from a Devonian carbonatite dyke, Kola peninsula, Russia: A record of geological evolution from the Archaean to the Palaeozoic. Lithos, 51:95~108.

Conticelli S, Avanzinelli R, Ammannati E, Casalini M. 2015. The role of carbon from recycled sediments in the origin of ultrapotassic igneous rocks in the central mediterranean. Lithos, 232: 174～196.

Corfu F, Hanchar J M, Hoskin P W O. 2003. Atlas of zircon textures. Reviews in Mineralogy & Geochemistry, 53(1):469～500.

Deng Jinfu, Feng Yanfang, Di Yongjun, Liu Cui, Xiao Qinghui, Su Shangguo, Zhao Guochun, Meng Fei, Che Rufeng. 2015a&. The intrusive spatial — temporal evolutional framework in the Paleo — Asian tectonic domain. Geological Review, 61(6):1211～1224.

Deng Jinfu, Feng Yanfang, Di Yongjun, Liu Cui, Xiao Qinghui, Su Shangguo, Zhao Guochun, Meng Fei, Ma Shuai, Yao Tu. 2015b&. Magmatic arc and ocean — continent transition: Discussion. Geological Review, 61(3): 473～484.

Ding Lixue, Ma Changqian, Li Jianwei. 2011. Timing and genesis of the adakitic and shoshonitic intrusions in the laoniushan complex, southern margin of the north China Craton: Implications for post-collisional magmatism associated with the qinling orogen. Lithos, 126(3～4): 212～232.

Ebert E, Grove T L. 2004. Phase relationships of a Tibetan shoshonite lava: Constraints on the melting conditions and the source rock. Lithos, 73(1～2): S31.

Elliott T, Plank T, Zindler A, White W, Bourdon B. 1997. Element transport from slab to volcanic front at the Mariana arc. J. Geophys. Res., 102(B7): 14991～15019.

Foley S, Peccerillo A. 1992. Potassic and ultrapotassic magmas and their origin. Lithos, 28(3～6):181～185.

Fan Yuxu, Li Tingdong, Xiao Qinghui, Cheng Yang, Li Yan, Guo Lingjun, Luo Pengyue. 2019&. Zircon U-Pb ages, geochemical characteristics of Late Permian granite in West Ujimqin Banner, Inner Mongolia, and tectonic significance. Geological Review, 65 (1):248～266.

Furman T and Graham D. 1999. Erosion of lithospheric mantle beneath the East African Rift system: Geochemical evidence from the Kivu volcanic province. Developments in Geotectonics, 24:237～262.

Jahangiri A, Fadaeian M, Songjian A. 2016. Geochemistry and emplacement of post-collisional shoshonitic dyke swarms, NW of Iran. Acta Geologica Sinica(English Edition), 90(S1): 99.

Jia Xiaohui, Wang Xiaodi, Yang Wenqiang, Niu Zhijun. 2017&. An overview of studies on shoshonitic socks. Geological Review, 63 (6):1587～1601.

Jian Ping, Liu Dunyi, Kroner A. 2010. Evolution of a Permian intraoceanic arc—trench system in the Solonker suture zone, Central Asian orogenicBelt, China and Mongolia. Lithos, 118:169～190.

Jian Ping, Kroner A, Windley B F, Shi Yuruo, Zhang Wei, Zhang Liqiao, Yang Weiran. 2012. Carboniferous and Cretaceous mafic—ultramafic massifs in Inner Mongolia (China): A SHRIMP zircon and geochemical study of the previously presumed integral "Hegenshan ophiolite". Lithos, 142～143: 48～66.

Jiang Yaohui, Jiang Shaoyong, Ling Hongfei, Zhou Xunruo, Rui Xingjian, Yang Wanzhi. 2002. Petrology and geochemistry of shoshonitic plutons from the western Kunlun orogenic belt, Xinjiang, northwestern China: Implications for granitoid geneses. Lithos, 63(3～4), 165～187.

Kang Jianli, Xiao Zhibin, Wang Huichu, Chu Hang, Ren Yunwei, Liu Huan, Gao Zhirui, Sun Yiwei. 2016&. Late Paleozoic subduction of the Paleo — Asian Ocean: Geochronological and geochemical evidence from the meta-basic volcanics of Xilinhot, Inner Mongolia. Acta Geologica Sinica, 90(2):383～397.

Li Gangzhu, Wang Yujing, Li Chengyuan. 2017#. Discovery of Early Permian radiolarian fauna in the Solon Obo ophiolite belt, Inner Mongolia and its geological significance. Chin. Sci. Bull., 62: 400～406.

Li Hongying, Zhou Zhiguang, Zhang Da, Li Pengju. 2015&. Geochronology, geochemistry and geological significance of Late Triassic rhyolites in Geerchulu, Xi Ujimqin Qi, Inner Mongolia. Bulletin of Mineralogy, Petrology and Geochemistry, 34(3):546～555.

Li Ke, Zhang Zhicheng, Li Jianfeng, Tang Wenhao, Feng Zhishuo, Li Qiugen. 2012&. Zircon SHRIMP U-Pb age and geochemical characteristics of the Mesozoic volcanic rocks in Xi Ujimqin Banner, Inner Mongolia. Geological Bulletin of China, 31(5):671～685.

Li Shuguang, Nie Y H, Xiao Y L, Zheng Y F, Jagoutz E. 1997#. Recycling of subducted continental crust of Dabie Mountain: Geochemical evidence. Science in China, 27(5): 412～418.

Li Shichao, Xu Zhongyuan, Liu Zhenghong, Li Yongfei. 2013&. Zircon U-Pb dating and geochemical study of volcanic rocks in Manitu Formation of central Da Hinggan Mountains. Geological Bulletin of China, 32(2～3):399～407.

Li Yingjie, Wang Genhou, Santosh M, Wang Jinfang, Dong Peipei, Li Hongyang. 2018c. Supra-subduction zone ophiolites from Inner Mongolia, North China: Implications for the tectonic history of the southeastern Central Asian Orogenic Belt. Gondwana Research, 59: 126～143.

Li Yingjie, Wang Jinfang, Li Hongyang and Dong Peipei. 2012&. Recognition of Diyanmiao ophiolite in Xi Ujimqin Banner, Inner Mongolia. Acta Petrologica Sinica, 28(4):1282～1290.

Li Yingjie, Wang Jinfang, Li Hongyang and Dong Peipei. 2015&. Recognition of Meilaotewula ophiolite in Xi Ujimqin Banner, Inner Mongolia. Acta Petrologica Sinica, 31(5):1461～1470.

Li Yingjie, Wang Jinfang, Li Hongyang and Dong Peipei. 2018b&. Discovery and significance of the Dahate fore — arc basalts from Diyanmiao ophiolite in Inner Mongolia. Acta Petrologica Sinica, 34 (2):469～482.

Li Yingjie, Wang Jinfang, Wang Genhou, Dong Peipei, Li Hongyang, Hu Xiaojia. 2018a. Discovery of the Plagiogranites in the Diyanmiao Ophiolite, Southeastern Central Asian Orogenic Belt, Inner Mongolia, China, and its tectonic significance. Acta Geologica Sinica(English Edition), 92(2):568～585.

Liu Hongtao, Zhai Mingguo, Liu Jianming and Sun Shihua. 2002&. The Mesozoic granitoids in the northern marginal region of North China Craton evolution from post-collisional to anorogenic settings. Acta Petrologica Sinica, 18(4):433～448.

Liu Jianfeng, Chi Xiaoguo, Zhang Xingzhou, Ma Zhihong, Zhao Zhi, Wang Tiefu, Hu Zhaochu, Zhao Xiuyu. 2009&. Geochemical characteristic of Carboniferous quartz diorite in the southern Xiwuqi area, Inner Mongolia and its tectonic significance. Acta Geologica Sinica, 83(3):365～376.

Liu Jianfeng, Li Jinyi, Chi Xiaoguo, Qu Junfeng, Hu Zhaochu, Fang Shu, Zhang Zhong. 2013. A Late Carboniferous to early Early — Permian subduction — accretion complex in Daqing pasture, southeastern Inner Mongolia: Evidence of northward subduction beneath the Siberian paleoplate southern margin. Lithos, 177(2):285～296.

Liu Rui, Yang Zhen, Xu Qidong, Zhang Xiaojun, Yao Chunliang. 2016&. Zircon U-Pb ages, elemental and Sr — Nd — Pb isotopic geochemistry of the Hercynian granitoids from the southern segment of the Da Hinggan Mts.: Petrogenesis and tectonic implications. Acta Petrologica Sinica, 32(5):1505～1528.

Lü Hongbo, Feng Xuedong, Wang Jun, Zhu Xiaoqing, Dong Xiaopeng, Zhang Haichun, Zhang Yuxu. 2018&. Ophiolitic Mélanges found in mount Langshan as the crucial evidence of collisional margin between North China Craton and Central Asian Orogenic Belt. Geological Review, 64(4): 777～805.

Massonne H J. 1992. Evidence for low — temperature ultrapotassic siliceous fluids in subduction zone environments from experiments in the system K_2O — MgO — Al_2O_3 — SiO_2 — H_2O (KMASH). Lithos, 28: 421～434.

Miao Laicheng, Fan Weiming, Liu Dunyi, Zhang Fuqin, Shi Yuruo and Guo Feng. 2008. Geochronology and geochemistry of the Hegenshan ophiolitic complex: Implications for late — stage tectonic evolution of the Inner Mongolia — Daxinganling Orogenic Belt, China. Journal of Asian Earth Sciences, 32(5～6): 348～370.

Middlemost E A K. 1994. Naming materials in the magma/igneous rock system. Earth Sci. Rev., 37: 215～224.

Miller C, Schuster R, Klotzli U, Frank W, Purtscheller F. 1999. Post-collisional potassic and ultrapotassic magmatism in SW Tibet: Geochemical and Sr — Nd — Pb — O isotopic constraints for mantle source characteristics and petrogenesis. J. Petrol., 40(9): 1399～1424.

Morrison G W. 1980. Characteristics and tectonic setting of the shoshonite rock association. Lithos, 13(1): 97～108.

Müller D, Groves D I. 2000. Potassic Igneous Rocks and Associated Gold — Copper Mineralization: 3rd ed. Berlin: Springer — Verlag: 1～266.

Müller D, Rock N M S, Groves D I. 1992. Geochemical discrimination between shoshonitic and potassic volcanic rocks in different tectonic settings: A pilot study. Mineralogy & Petrology, 46(4): 259～289.

Nima Ciren, Wang Guocan, Dun Du, Ciren Yangzong. 2015&. Petrology, geochemistry and zircon U-Pb age of high potassic shoshonitic volcanic rocks in Shiquanhe area, Tibet. Geological Bulletin of China, 34(9): 1656～1667.

Othman D B, White W M, Patchett J. 1989. The geochemistry of marine sediments, island arc magma genesis, and crust—mantle recycling. Earth Planet. Sci. Lett., 94(1～2): 1～21.

Pearce J A, Peate D W. 1995. Tectonic implications of the composition of volcanic arc magmas. Ann. Rev. Earth Planet. Sci., 23: 251～285.

Peccerillo A, Taylor S R. 1976. Geochemistry of eocene calc—alkaline volcanic rocks from the Kastamonu Area, Northern Turkey. Contributions to Mineralogy and Petrology, 58: 63～81.

Pe-Piper G, Zhang Y, Piper D J W & Prelevic D. 2014. Relationship of mediterranean type lamproites to large shoshonite volcanoes, Miocene of Lesbos, Ne Aegean Sea. Lithos, 184～187(1): 281～299.

Qiu Jiansheng, Xu Xisheng, Jiang Shaoyong. 2003&. Deep subduction of crust materials and its implication to the genesis of potash-rich volcanic rocks. Earth Science Frontiers, 10(3): 191～200.

Qiu Jiansheng, Liu Liang, Li Youlian, Zhao Jiaolong. 2013&. Petrogenesis of potassic volcanic rocks in the middle—south parts of the Yishu deep fault zone: Constraints from elemental geochemistry and Sr — Nd — Hf isotopes. Acta Geologica Sinica, 87(9): 1193～1210.

Qiu Jiansheng, Wang Dezi, Liu Hong and Ling Wenli. 2002&. Post-collisional potash-rich volcanic rocks in the north margin of Dabie orogenic belt: Geochemistry and petrogenesis. Acta Petrologica Sinica, 18(3): 319～330.

Sengor A M C, Natalin B A, Burtman V S. 1993. Evolution of the Altaid tectonic collage and Paleozoic crustal growth in Eurasia. Nature, 364: 299～307.

Shi Yuruo, Liu Dunyi, Zhang Qi, Jian Ping, Zhang Fuqin, Miao Laicheng, Zhang Lüqiao. 2007&. SHRIMP U-Pb zircon dating of Triassic A-type granites in Sonid Zuoqi, central Inner Mongolia, China, and its tectonic implications. Geological Bulletin of China, 26(2): 183～189.

Squire R J, Crawford A J. 2007. Magmatic characteristics and geochronology of Ordovician igneous rocks from the Cadiaa Neville region, New South Wales: Implications for tectonic evolution. Journal of the Geological Society of Australia, 54(2～3): 293～314.

Sun Chihhsien, Stern R J. 2001. Genesis of Mariana shoshonites: Contribution of the subduction component. J. Geophys. Res., 106 (B1): 589～608.

Sun S-S, Mcdonough W F. 1989. Chemical and isotopic systematics of oceanic basalt: Implication for mantle composition and processes. Geol. Soc. London Spec. Pub., 42: 313～345.

Tian Shugang, Li Zishun, Zhang Yongsheng, Gong Yuexuan, Zhai Daxing, Wang Meng. 2016&. Late Carboniferous — Permian tectono—geographical conditions and development in Eastern Inner Mengolia and adjacent areas. Acta Geologica Sinica, 90(4): 688～707.

Turner S, Arnaud N, Liu J, Rogers N, Hawkesworth C, Harris N, Kelley S, Calsteren P V, Deng W M. 1996. Post-collisional shoshonitic volcanism on the Tibetan plateau: Implications for convective thinning of the lithosphere and the source of ocean island basalts. J. Petrol., 37: 45～71.

Wang Jinfang, Li Yingjie, Li Hongyang. 2017. Zircon LA-ICP-MS U-Pb age and island — arc origin of the Bayanhua gabbro in the Hegenshan suture zone, Inner Mongolia. Acta Geologica Sinica (English Edition), 91(6): 2316～2317.

Wang Jinfang, Li Yingjie, Li Hongyang and Dong Peipei. 2017a&. Discovery of Early Permian intra-oceanic arc adakite in the Meilaotewula ophiolite, Inner Mongolia and its evolution model. Acta Geologica Sinica, 91(8): 1776～1795.

Wang Jinfang, Li Yingjie, Li Hongyang and Dong Peipei. 2017b&. LA-ICP-MS zircon U-Pb dating of the Nuhete Early Cretaceous A-type granite in Xi Ujimqin Banner of Inner Mongolia and its geological significance. Geological Bulletin of China, 36(8): 1343～1358.

Wang Jinfang, Li Yingjie, Li Hongyang and Dong Peipei. 2018b&. Zircon U-Pb dating of the Shijiangshan Late Jurassic—Early Cretaceous A-type granite in Xiwuqi, Inner Mongolia and its tectonic setting. Geological Bulletin of China, 37(2～3): 382～396.

Wang Jinfang, Li Yingjie, Li Hongyang and Dong Peipei. 2018c&. Zircon U-Pb dating of the Wulangou adakite, Inner Mongolia and its tectonic setting. Geological Bulletin of China, 37(10): 1933～1943.

Wang Jinfang, Li Yingjie, Li Hongyang and Dong Peipei. 2018a&. The discovery of the Early Permian high-Mg diorite in Meilaotewula SSZ ophiolite of Inner Mongolia and its intra-oceanic subduction. Geology in China, 45(4): 706～719.

Wang Jinfang, Li Yingjie, Li Hongyang, Dong Peipei. 2019&. Zircon U-Pb ages and geochemical characteristics of Baiyinhushu trondhjemite in Hegenshan suture zone and their tectonic implications. Geological Review, 65(4): 857～872.

Wang Jinfang, Li Yingjie, Li Hongyang, Dong Peipei. 2020a&. Late Carboniferous intraoceanic subduction of the Paleo-Asian Ocean: New evidences from the Zagayin high-Mg andesite in the

Meilaotewula SSZ ophiolite. Geological Review, 66(2): 289~306.

Wang Jinfang, Li Yingjie, Li Hongyang, Dong Peipei. 2020b&. Paleo-Asian Ocean subducted slab breakoff and post orogenic extension: Evidence from geochronology and geochemistry of volcanic rocks in the Hegenshan suture zone. Acta Geologica Sinica, 94(12): 3561~3580.

Wang Jinfang, Li Yingjie, Li Hongyang, Dong Peipei. 2021&. Late Carboniferous TTG magmatic event in the Hegenshan suture zone: Zircon U-Pb geochronology and geochemical constraints from the Huduge trondhjemite. Acta Geologica Sinica, 95(2): 396~412.

Wang Liangyu, Liao Q A, Jiang Y C, Luo T, Hu C B, Xiao D, Liu Y. 2016&. Petrogenesis and tectonics of late Early Cretaceous Shoshonitic volcanic rocks in Xilin Hot, Inner Mongolia. Geological Bulletin of China, 35(6): 919~931.

Wang Shuqing, Hu Xiaojia, Yang Zeli, Zhao Hualei, Zhang Yong, Hao Shuang, He Li. 2018&. Geochronology, geochemistry, Sr — Nd — Hf isotopic characteristics and geological significance of Carboniferous Yuejin arc intrusive rocks of Xilinhot, Inner Mongolia. Earth Science, 43(3): 1~31.

Wang Xiang. 2018&. Analysis on the oreforming time and genesis of the Bayan Obo REE — Nb — Fe deposit: With a discussion on the mass extinction at the P — T boundary and "AMH Orogeny". Geological Review, 64(2): 299~345.

Williams H M, Turner S P, Pearce J A, Kelley S P, Harris N B W. 2004. Nature of the source regions for post-collisional, potassic magmatism in southern and northern Tibet from geochemical variations and inverse trace element modelling. J. Petrol., 45: 555~607.

Windley B F, Alexeiev D, Xiao W J, Kroner F, Badarch G. 2007. Tectonic models for accretion of the Central Asian Orogenic Belt. Journal of the Geological Society, 164(1): 31~47.

Wyborn D. 1992. The tectonic significance of Ordovician magmatism in the eastern Lachlan Fold Belt. Tectonophysics, 214(1~4): 177~192.

Xiao Wenjiao, Windley B F, Hao Jie, Zhai Mingguo. 2003. Accretion leading to collision and the Permian Solonker suture, Inner Mongolia, China: Termination of the central Asian orogenic belt. Tectonics, 22 (6): 1069~1089.

Xiao Wenjiao, Windley B F, Huang B C. 2009. End — Permian to mid — Triassic termination of the accretionary processes of the southern Altaids: Implications for the geodynamic evolution, Phanerozoic continental growth, and metallogeny of Central Asia. Int. J. Earth Sci., 98: 1189~1217.

Xu Xinxue, Li Junjian, Liu Junchang, Xin Jianwei, Dai Tao, Niu Yongqiang, Zhang Li. 2011#. The crust—upper mantle electrical structure along Xilinhot — Dongwuqi section. Chinese J. Geophys., 54 (5): 1301~1309.

Xue Huaimin, Ma Fang, Cao Guangyue. 2015. Geochronology and petrogenesis of shoshonitic igneous rocks, Luzong volcanic basin, middle and lower Yangtze River reaches, China. Journal of Asian Earth Sciences, 110: 123~140.

Xue Xiaogang, Zhou Changhong, Zhang Xuebin, Li Caihong. 2018&. Zircon U-Pb dating and geochemical characteristics of volcanic rocks in the Meiletu Formation of eastern Xilin Gol League, Inner Mongolia and their geological implications. Geology and Exploration, 54 (5): 957~967.

Yang Huaben, Wang Wendong, Yan Yongsheng, Wei Xiaoyong, Ceng Chengbao. 2016&. Origin of basalts of the Tamulangou Formation and mantle enrichment in Xinlin area, northern Greater Hinggan Mountains. Geological Review, 62(6): 1471~1486.

Yuan Jianguo, Gu Yuchao, Xiao Rongge, Qu Yunyan, Duan Kaibo, Han Yue. 2017&. Geochemistry and zircon U-Pb dating of granites in Early Cretaceous in eastern Xilin Hot, Inner Mongolia and its geological implications. Geoscience, 31(6): 1131~1146.

Zhang Bangtong, Wu Junqi, Ling Hongfei, Chen Peirong. 2011&. Elemental geochemical evidence for genesis of intraplate shoshonite and mantle-derived fluid metasomatism: Shoshonite from Huichang, Southern Jiangxi Province as an example. Geochimica, 40(5): 443~453.

Zhang Xiaohui, Zhang Hongfu, Tang Yanjie, Liu Jianming. 2006&. Early Triassic A-type felsic volcanism in the Xilinhaote — Xiwuqi, central Inner Mongolia: Age, geochemistry and tectonic implications. Acta Petrologica Sinica, 22(11): 2769~2780.

Zhang Xiangxin, Gao Yongfeng, Lei Shihe. 2016&. Ziron U-Pb age and geochemistry of shoshonitic rocks from the Manitu Formation in the Honggeer area, central Inner Mongolia and their geological significance. Geochimica, 45(4): 356~373.

Zhang Xuebin, Zhou Changbong, Lai Lin, Xu Cui, Tian Ying, Chen Lichen, Wei Min. 2015&. Geochemistry and zircon U-Pb dating of volcanic rocks ineastern Xilin Hot, Inner Mongolia and their geological implications. Geology and Exploration, 51(2): 290~302.

Zhang Zhicheng, Li Ke, Li Jianfeng, Tang Wenhao, Chen Yan, Luo Zhiwen. 2015. Geochronology and geochemistry of the Eastern Erenhot ophiolitic complex: Implications for the tectonic evolution of the Inner Mongolia — Daxinganling Orogenic Belt. J. Asian Earth Sci., 97(B): 279~293.

Zhang Zhaochong, Xiao Xuchang, Wang Jun, Wang Yong, Kusky T M. 2008. Post-collisional Plio — Pleistocene shoshonitic volcanism in the western Kunlun Mountains, NW China: Geochemical constraints on mantle source characteristics and petrogenesis. J. Asian Earth Sci., 31(4~6): 379~403.

The Asagetu shoshonitic volcanic rocks in the Hegenshan Suture: Zircon LA-ICP-MS U-Pb ages, geochemical features and its tectonic significance

WANG Jinfang, LI Yingjie, LI Hongyang, DONG Peipei

College of Earth Sciences, Hebei GeoUniversity, Shijiazhuang, 050031

Objectives: The Hegenshan suture of the eastern Central Asian Orogenic Belt (CAOB) has developed the Late Paleozoic SSZ type ophiolites—arc magmatic rocks and Mesozoic volcanic rocks. The spatial temporal distribution and genetic relationship between Mesozoic volcanic rocks and late Paleozoic ophiolite—arc magmatic rocks have gradually become one of the important scientific issues in the tectonic evolution of the Hegenshan suture. Therefore, this study carried out zircon geochronology, geochemistry, genesis and tectonic environment on the Asagetu Mesozoic volcanic rocks in order to provide new evidence for the tectonic evolution of the Hegenshan suture.

Methods: Based on field geological surveying, petrology, geochemistry and LA-ICP-MS zircon U-Pb geochronology of the Asagetu volcanic rocks exposed in the sothern part of the Diyanmiao ophiolitic melange belt of the Hegenshan suture in Xiwuqi of Inner Mongolia, this paper discusses petrogenesis and tectonic environment of the volcanic rocks, and slab breakoff—post orogenic extension of the Paleo-Asian Ocean.

Results: The Asagetu volcanic rocks are mainly composed of trachyandesite, trachyte and trachydacite. Zircon LA-ICP-MS U-Pb dating for the trachyandesite volcanic rocks shows that the age of volcanic rocks is 132.1±0.7Ma. Petrogeochemistry shows that volcanic rocks belong to shoshonite series. Rocks with high Na_2O+K_2O (7.61%~10.35%), K_2O (3.94%~6.04%), Al_2O_3 (16.32%~17.99%) and low TiO_2 (0.45%~0.95%) are obviously enriched in LILEs (Rb, Ba and U) and LREEs, and depleted in HFSEs (Nb, Ta and Ti). The contents of rare earth elements range from 109.62×10^{-6} to 174.68×10^{-6}. The chondrite normalized REE distribution patterns are of right inclined shape. Combined with the crust—upper mantle electrical structure and the temporal—spatial distribution of the Late Paleozoic ophiolites—arc magmatic rocks and Mesozoic post orogenic A-type granites in the Hegenshan suture, the geodynamic model of the subducted slab break off—post orogenic extension of the shoshonitic volcanic rocks has been preliminarily established.

Conclusions: This study determines the Early Cretaceous (132.1±0.7Ma) Asagetu volcanic rocks, which are related to the previous oceanic subduction and formed in the subsequent subducted slab break off—post orogenic extension tectonic setting. The fluids dehydrated from the subducted oceanic crust of the Paleo-Asian Ocean metasomatized the overlying mantle to form the enriched mantle of the Hegenshan suture. The subsequent subducted slab break off—the post orogenic extension triggered partial melting of the enriched mantle to produce the shoshonitic magma. The discovery and confirmation of the Asagetu shoshonitic rocks in the Early Cretaceous provide new evidence for the Paleo-Asian Ocean subducted slab break off—post orogenic extension.

Acknowledgements: This study was financially supported by the National Natural Science Foundation of China (grant No. 41972061) and the China Geological Survey (grants No. 1212011120711 and 1212011120701).

Keywords: Shoshonitic volcanic rocks; slab break off; post orogenic extension environment; Early Cretaceous; Hegenshan suture

First author: WANG Jinfang, female, born in 1983, associate professor, mainly engaged in petrology and geochemistry; Email: wjfb1983@163.com

Manuscript received on: 2020-01-23; Accepted on: 2021-03-07; Network published on: 2021-03-20

Doi: 10.16509/j.georeview.2021.03.075 **Edited by**: ZHANG Yuxu